Photoproduction of $\bar{D}^0\Lambda_c^+$ within the Regge-plus-resonance model

D. Skoupil[1,*] and Y. Yamaguchi[2,3]

[1]*Nuclear Physics Institute, CAS, Řež/Prague 25068, Czech Republic*
[2]*Advanced Science Research Center, Japan Atomic Energy Agency (JAEA), Tokai 319-1195, Japan*
[3]*Nishina Center for Accelerator-Based Science, RIKEN, Wako 351-0198, Japan*

(Received 14 July 2020; accepted 10 September 2020; published 12 October 2020)

$\bar{D}^0$-meson photoproduction off the proton is studied at energies from the process threshold up to 20 GeV. The background part of the process is modeled within the Regge model with the help of $\bar{D}^0$-meson trajectories that are being exchanged in the t channel or Λ_c^+-baryon trajectories exchanged in the u channel. These contributions create cross sections which are smooth functions of energy. The introduction of exchanges of three hidden-charm pentaquarks with spin $1/2$ and $3/2$ in the s channel then creates sharp peaks in the cross section predictions. In order to account for the finite size of the particles involved, we introduce hadron form factors. In analysis of model predictions with pseudoscalar and pseudovector couplings in the strong vertex, the contact term was shown to play a non-negligible role. A great merit of the proposed approach is its limited number of parameters that need to be adjusted as there are to this date no data available for this process. Being limited by the broken SU(4) symmetry and guided by other works that show their predictions of this process, we could adjust the parameters manually in order to provide at least qualitative results.

DOI: 10.1103/PhysRevD.102.074009

I. INTRODUCTION

Hadrons with heavy flavor provide new phenomena in the hadron physics. Many exotic hadrons such as the X, Y, Z states and the hidden-charm pentaquark P_c have been reported in the accelerator facilities [1–4]. The properties of these states cannot be explained by the ordinary hadron picture, baryons as three quark states and mesons as quark-antiquark states, while they are expected to have exotic structures, e.g., the multiquark states and hadronic molecules. The heavy baryons can be good probes to investigate the diquark degrees of freedom inside the baryons, where the heavy baryon is interpreted as a bound state of a heavy quark and a light diquark for single-heavy baryons, and of a heavy diquark and a light quark for double-heavy baryons [5–8]. The separation of the light degrees of freedom, i.e., the light-quark spins and orbital angular momenta, from the heavy-quark spins results in a novel symmetry in the heavy-quark sector, which is the heavy-quark spin symmetry [4,9–14]. This symmetry appears because the spin-flip interaction of the heavy quark is suppressed by a factor of $1/m_Q$ with the heavy-quark mass m_Q.

In the experimental studies, the heavy hadrons have been investigated at various accelerator facilities [2,15] such as the e^+e^- collision experiments in Belle, *BABAR* [16] and BESIII [17], and the heavy ion collisions in LHCb [18–27]. The photoproduction of the charmed hadrons was performed in Jefferson Lab [28,29]. As a proposal, the charmed hadron production induced by the pion beam is planned in Japan Proton Accelerator Research Complex [30].

The P_c state is one of the interesting topics in the heavy-hadron physics which has impacted the studies of the exotic states. The P_c resonances were reported by the LHCb Collaboration in the weak decay $\Lambda_b \to J/\psi \bar{K}$ [20–23]. The minimal quark content of the P_c states is assumed to be $c\bar{c}uud$, and thus it is called the hidden-charm pentaquark. In the first observation in 2015 [20–22], LHCb reported the twin resonances $P_c(4380)$ and $P_c(4450)$ at $4380 \pm 8 \pm 29$ MeV and $4449.8 \pm 1.7 \pm 2.5$ MeV, respectively. The $P_c(4380)$ was found below the $\bar{D}\Sigma_c^*$ threshold and with the large decay width $\Gamma = 205 \pm 18 \pm 86$ MeV, while the $P_c(4450)$ was below the $\bar{D}^*\Sigma_c$ threshold and with the narrow decay width $\Gamma = 39 \pm 5 \pm 19$ MeV. In 2019, a new analysis with more statistical data was performed [23], where three narrow peaks were reported as summarized in Table I. The two peaks were found at 4440 and 4457 MeV and called $P_c(4440)$ and $P_c(4457)$ resonances, respectively, where the $P_c(4450)$ reported in 2015 was resolved into the two peaks. The other peak was a new one which was found at 4312 MeV, below the $\bar{D}\Sigma_c$ threshold, and called $P_c(4312)$. For the broad resonance $P_c(4380)$, however, the data can be fitted well without the Breit-Wigner contributions corresponding to the $P_c(4380)$ in the new analysis. The P_c resonances were also studied in the $\gamma p \to J/\psi p$ reaction by the GlueX Experiment in Hall D at

*Corresponding author.
skoupil@ujf.cas.cz

TABLE I. Properties of the three pentaquark states assumed in Ref. [23]. The quantum numbers of P_c's have not been determined in experiments yet, while the total angular momentum J and parity P shown in the table are predicted in Ref. [66].

Particle	Mass [MeV]	Width [MeV]	J^P (pred.)
$P_c^+(4312)$	$4311.9 \pm 0.7^{+6.8}_{-0.6}$	$9.8 \pm 2.7^{+3.7}_{-4.5}$	$1/2^-$
$P_c^+(4440)$	$4440.3 \pm 1.3^{+4.1}_{-4.7}$	$20.6 \pm 4.9^{+8.7}_{-10.1}$	$3/2^-$
$P_c^+(4457)$	$4457.3 \pm 0.6^{+4.1}_{-1.7}$	$6.4 \pm 2.0^{+5.7}_{-1.9}$	$1/2^-$

Jefferson Lab [28]. However, no clear contributions from the P_c states were found. In the theoretical studies, there have been many works of the hidden-charm pentaquarks as the compact states, hadronic molecules, kinematical effects, etc. [31–67]. The contributions from the P_c states in the cross sections have also been discussed for the photoproduction [68–74], the electroproduction [75], and the reactions induced by pion beams [76–79].

The interesting phenomena show up in the heavy-quark sector, which have not appeared in the light-quark sectors. However, we do not achieve to understand the properties of the heavy baryons which are the hadron structures as well as the quantum numbers such as the spin and parity. Further experimental and theoretical studies are necessary to study nature of the heavy hadrons.

In this paper, we study the photoproduction cross section of the $\gamma p \to \bar{D}^0 \Lambda_c^+$ reaction, where the contributions of the hidden-charm pentaquarks $P_c^+(4312)$, $P_c^+(4440)$, and $P_c^+(4457)$ are included as the intermediate states of the reaction. The photoproduction experiments provide further results for the properties of charmed hadrons including the P_c states explored in the LHCb experiment. Since the photoproduction process with the intermediate exotic states does not satisfy the condition of anomalous triangle singularity [70], the experiment can be utilized as a tool for investigating exotic states. We use the masses and decay widths of $P_c^+(4312)$, $P_c^+(4440)$, and $P_c^+(4457)$ given by LHCb [23] summarized in Table I. The spin (J) and parity (P) are not determined in experiments yet. In Ref. [66], the P_c states were studied as the hadronic molecules of $\bar{D}^{(*)}\Lambda_c - \bar{D}^{(*)}\Sigma_c^{(*)}$, where the one-pion exchange potential as the long-range force, and the coupling to the five-quark states working as the short-range force were employed. The J^P is assigned as $1/2^-$ for $P_c^+(4312)$, $3/2^-$ for $P_c^+(4440)$, and $1/2^-$ for $P_c^+(4457)$ in [66], where the same assignment was also given in [59]. Assuming the P_c states as the hadronic molecules of $\bar{D}^{(*)}\Lambda_c - \bar{D}^{(*)}\Sigma_c^{(*)}$, these states strongly couple to open-charm channels such as $\bar{D}^{(*)}\Lambda_c$ and $\bar{D}^{(*)}\Sigma_c^{(*)}$ rather than hidden-charm ones such as $J/\psi p$, because the coupling between the P_c and hidden-charm states is induced by exchanges of the charmed hadrons (or the charm quark) having large masses.

The framework which we employ in this paper for studying photoproduction of $\bar{D}^0\Lambda_c^+$ was previously used for analyzing photoproduction of $K^+\Lambda$ [80] where it led to a good agreement with experimental data. As the process of $\bar{D}^0\Lambda_c^+$ photoproduction off proton is analogous to the $K^+\Lambda$ photoproduction off proton, we can employ the same techniques here as well. This method is called the Regge-plus-resonance model, originally constructed by a group at Ghent University [81], and allows to describe the photoproduction process in the threshold region as well as at higher energies. The Regge part of the amplitude, which is a smooth function of energy, creates the background in the threshold region and constitutes the whole prediction above this region. On top of this background, we add a few pentaquark exchanges which create a peak structure above the threshold. An essential merit of the Regge-plus-resonance approach is its small number of free parameters.

In our framework, the $\gamma D^0 D^0$ coupling is introduced in the exchange of $\bar{D}^0$-meson trajectory in the t channel. In naive expectations, the photon does not couple to neutral mesons. However, the open-flavor structure of the $\bar{D}^0$ meson composed of $\bar{c}$ and u quarks yields the nonzero $\gamma D^0 D^0$ coupling as long as the flavor SU(4) symmetry is broken, while the $\gamma D^0 D^0$ coupling vanishes in the flavor SU(4) limit. We derive the effective $\gamma D^0 D^0$ coupling by introducing the vector meson dominance (VMD) [82,83], where the photon couples to the $\bar{D}^0$ mesons via the neutral vector-meson propagator.

This paper is organized as follows. In Sec. II, we present various models which give us hints on the values of the couplings in the strong vertex and we show the course of the calculation together with the method used in the current study, i.e., the Regge-plus-resonance model. In Sec. III, the results are shown and discussed with emphasis on the type of coupling in the strong vertex and values of coupling constants. Finally, Sec. IV concludes this paper. Details on effective couplings of a photon and D mesons are given in the Appendix A.

II. METHODOLOGY

Most of the knowledge on the DN interaction comes from calculations using hadronic Lagrangians motivated by SU(4) extensions of light-flavor chiral Lagrangians and heavy-quark symmetry. Otherwise, there is no experimental information on the DN interaction currently available (situation may change with the PANDA@FAIR experiment 84]]). For the strong coupling constant $g_{D\Lambda_c^+ N}$, we could use the SU(4) flavor symmetry as a reasonable first approximation and relate this coupling constant to other couplings in the light-flavor sector,

$$g_{D\Lambda_c^+ N} = g_{K\Lambda N} = -\frac{3 - 2\alpha_D}{\sqrt{3}} g_{\pi NN}, \tag{1}$$

where $g_{\pi NN}^2/4\pi = 14.4$ and $\alpha_D = 0.644$. The relation between $g_{K\Lambda N}$ and $g_{\pi NN}$ is taken from Ref. [85]. This gives

us $g_{D\Lambda_c^+N}/\sqrt{4\pi} = -3.75$ and when we assume the SU(4) flavor symmetry being broken at the level of 20%, we get

$$-4.5 \leq \frac{g_{D\Lambda_c^+N}}{\sqrt{4\pi}} \leq -3.0.$$

Besides employing the SU(4) symmetry, one can use QCD sum rules (QCDSR) and obtains values which are quite different, i.e.,

$$g_{D\Lambda_c^+N} \sim 6.7 - 7.9.$$

The coupling constant for the $D^{(*)}\Lambda_c^+N$ vertex, $g_{D^{(*)}\Lambda_c^+N}$, has been investigated by using various methods. These values are unfortunately not consistent with each other, as summarized in Table II. The coupling constants $g_{D\Lambda_c^+N}$ and $g_{D^*\Lambda_c^+N}$ in Table II are defined as

$$\langle \Lambda_c(p')|D(q)N(p)\rangle = g_{D\Lambda_c^+N}\bar{u}_{\Lambda_c}(p')i\gamma_5 u_N(p), \tag{2}$$

$$\langle \Lambda_c(p')|D^*(q)N(p)\rangle = \bar{u}_{\Lambda_c}(p')(g^V_{D^*\Lambda_c^+N}\varepsilon\cdot\gamma + ig^T_{D^*\Lambda_c^+N}\sigma_{\mu\nu}\varepsilon^\mu q^\nu)u_N(p). \tag{3}$$

We note that the definitions of the coupling constant are different in references.

We can again employ the SU(4) symmetry and relate this coupling to the known coupling $g_{\rho NN} = 3.25$, i.e., $g_{D^*\Lambda_c^+N} = -\sqrt{3}g_{\rho NN} = -5.63$. Assuming the SU(4) flavor violation, we get an interval

$$-6.8 \leq g_{D^*\Lambda_c^+N} \leq -4.5.$$

When using the QCD sum rules, we obtain for this coupling an approximate value $g_{D^*\Lambda_c^+N} \sim -7.5$.

According to Ref. [86], the $g_{D\Lambda_c^+N}$ must be larger than $g_{D^*\Lambda_c^+N}$.

The calculation procedure used in this paper is analogous to the one recently used in the $K^+\Lambda$ photoproduction study [92] as it is easily applicable for photoproduction of various pseudoscalar mesons. The invariant amplitude of the process

$$\gamma(k) + p(p) \to \bar{D}^0(p_D) + \Lambda_c^+(p_\Lambda),$$

where the corresponding four-momenta are shown in the parentheses and the four-momenta of the intermediate particles are denoted by q, can be decomposed into the linear combination of six covariant gauge-invariant contributions

$$\mathbb{M} = \sum_{j=1}^{6} \mathcal{A}_j(k^2, s, t, u)\bar{u}(p_\Lambda)\gamma_5\mathcal{M}_j u(p), \tag{4}$$

where $\mathcal{M}_j$ are explicitly gauge-invariant operators

$$\mathcal{M}_1 = (\not{k}\not{\varepsilon} - \not{\varepsilon}\not{k})/2, \tag{5a}$$

$$\mathcal{M}_2 = p\cdot\varepsilon - k\cdot p\, k\cdot\varepsilon/k^2, \tag{5b}$$

$$\mathcal{M}_3 = p_\Lambda\cdot\varepsilon - k\cdot p_\Lambda\, k\cdot\varepsilon/k^2, \tag{5c}$$

$$\mathcal{M}_4 = \not{\varepsilon}k\cdot p - \not{k}p\cdot\varepsilon, \tag{5d}$$

$$\mathcal{M}_5 = \not{\varepsilon}k\cdot p_\Lambda - \not{k}p_\Lambda\cdot\varepsilon, \tag{5e}$$

$$\mathcal{M}_6 = \not{k}k\cdot\varepsilon - \not{\varepsilon}k^2, \tag{5f}$$

and ε_μ is the polarization vector of the photon. The scalar amplitudes $\mathcal{A}_j(k^2, s, t, u)$ contain contributions from all of the considered Feynman diagrams. The expressions of $\mathcal{A}_j$ amplitudes for various particle exchanges are shown in subsequent sections.

We note that the formalism shown here is given as the general one which can be applied to the production both with the virtual and real photons corresponding to the electroproduction and photoproduction, respectively. The photoproduction can be viewed as a special case of the electroproduction when the incoming photon is on its mass shell and thus the terms k^2 and $\vec{k}\cdot\vec{\varepsilon}$ vanish. The decomposition of the amplitude to the invariant operators $\mathcal{M}_i$ used in our work is not unique as there can be found other bases in the literature, e.g., in Ref. [93]. The basis of ours and of Ref. [93] is equivalent and there also

TABLE II. Summary of the coupling constants $g_{D^{(*)}\Lambda_c^+N}$ obtained by using various methods: SU(4) symmetry, QCDSR, light-cone QCD sum rules (LCQCDSR), and quark model. For the $g_{D\Lambda_c^+N}$ coupling, we use the convention of Eq. (1).

Method	$g_{D\Lambda_c^+N}$	$g_{D^*\Lambda_c^+N}$	Reference
SU(4)	-13.2	(4.3, 6.07 GeV^{-1})	[86]
QCDSR	-6.74 ± 2.12	…	[87]
	-7.9 ± 0.9	-7.5 ± 1.1	[88]
	-4.82 ± 1.44	…	[89]
LCQCDSR	$-12.3^{+5.3}_{-4.2}$	$(-6.9^{+2.4}_{-2.9}, 1.3^{+0.87}_{-0.59}$ GeV$^{-1})$	[90]
Quark model	$(-16.95, -13.56)$	…	[91]

exists a transformation matrix between them. For instance, another basis for the invariant operators can be found in Refs. [94–96]. In Appendix B, we show the transformation between our basis and the basis of Levy *et al.* [95,96].

Further on, we use a representation of the Lorentz-invariant matrix element (4) in terms of the two-component spinor Chew, Goldberger, Low, and Nambu (CGLN) amplitudes [97,98]. In the c.m. frame, the Lorentz-invariant matrix element (4) can be rewritten as

$$\mathbb{J}^{\mu}\varepsilon_{\mu} = \chi_{\Lambda}^{+}\mathcal{F}\chi_{p}, \tag{6}$$

where χ_p and χ_Λ are the Pauli spinors of the proton and Λ_c^+ baryon and

$$\begin{aligned}\mathcal{F} = {} & f_1\vec{\sigma}\cdot\vec{\varepsilon} - \mathrm{i}f_2\vec{\sigma}\cdot\hat{\vec{p}}_D\vec{\sigma}\cdot(\hat{\vec{k}}\times\vec{\varepsilon}) \\ & + f_3\vec{\sigma}\cdot\hat{\vec{k}}\hat{\vec{p}}_D\cdot\vec{\varepsilon} + f_4\vec{\sigma}\cdot\hat{\vec{p}}_D\hat{\vec{p}}_D\cdot\vec{\varepsilon} \\ & + f_5\vec{\sigma}\cdot\hat{\vec{k}}\hat{\vec{k}}\cdot\vec{\varepsilon} + f_6\vec{\sigma}\cdot\hat{\vec{p}}_D\hat{\vec{k}}\cdot\vec{\varepsilon}.\end{aligned} \tag{7}$$

Here $\hat{\vec{k}} = \vec{k}/|\vec{k}|$, $\hat{\vec{p}}_D = \vec{p}_D/|\vec{p}_D|$, $\vec{\sigma}$ are the Pauli matrices, and $\vec{\varepsilon}$ is the spatial component of the photon polarization vector. The CGLN amplitudes $f_i(k^2, s, t, u)$ are expressed via the scalar amplitudes A_j,

$$f_1 = N^*[-(W-m_p)\mathcal{A}_1 + k\cdot p\mathcal{A}_4 + k\cdot p_\Lambda\mathcal{A}_5 - k^2\mathcal{A}_6], \tag{8a}$$

$$f_2 = N^*\frac{|\vec{k}||\vec{p}_D|}{(E_\Lambda^*+m_\Lambda)(E_p^*+m_p)}[(W+m_p)\mathcal{A}_1 + k\cdot p\mathcal{A}_4 + k\cdot p_\Lambda\mathcal{A}_5 - k^2\mathcal{A}_6], \tag{8b}$$

$$f_3 = -N^*\frac{|\vec{k}||\vec{p}_D|}{E_p^*+m_p}[\mathcal{A}_3 + (W+m_p)\mathcal{A}_5], \tag{8c}$$

$$f_4 = N^*\frac{|\vec{p}_D|^2}{E_\Lambda^*+m_\Lambda}[\mathcal{A}_3 - (W-m_p)\mathcal{A}_5], \tag{8d}$$

$$f_5 = N^*\frac{|\vec{k}|^2}{E_p^*+m_p}\left[\mathcal{A}_1 - \frac{1}{k^2}[(k^2+k\cdot p)\mathcal{A}_2 + k\cdot p_\Lambda\mathcal{A}_3] - (W+m_p)(\mathcal{A}_4+\mathcal{A}_6)\right], \tag{8e}$$

$$f_6 = N^*\frac{E_\gamma^*|\vec{k}||\vec{p}_D|}{(E_\Lambda^*+m_\Lambda)(E_p^*+m_p)}\left\{\mathcal{A}_1 - m_p\mathcal{A}_4 + \frac{k\cdot p_\Lambda}{E_\gamma^*}\mathcal{A}_5 + \frac{(E_p^*+m_p)}{E_\gamma^* k^2}[(k^2+k\cdot p)\mathcal{A}_2 + k\cdot p_\Lambda\mathcal{A}_3] - (W+m_p)\mathcal{A}_6\right\}, \tag{8f}$$

where $W = \sqrt{s}$, and E_p^* (m_p), E_Λ^* (m_Λ), E_D^* (m_D), and E_γ^* are the c.m. energies (masses) of the proton, charmed baryon, D meson, and photon, respectively. The normalization factor reads

$$N^* = \sqrt{\frac{(E_\Lambda^*+m_\Lambda)(E_p^*+m_p)}{4m_\Lambda m_p}}. \tag{9}$$

With help of the CGLN amplitudes, the differential cross section of the $\bar{D}^0$-meson photoproduction can be calculated as

$$\frac{d\sigma}{d\Omega} = C\,\mathrm{Re}\left\{|f_1|^2 + |f_2|^2 - 2f_1f_2^*\cos\theta_D + \sin^2\theta_D\left[\frac{1}{2}(|f_3|^2+|f_4|^2) + f_1f_4^* + f_2f_3^* + f_3f_4^*\cos\theta_D\right]\right\}, \tag{10}$$

where the normalization factor C reads

$$C = (\hbar c)^2\frac{\alpha}{4\pi}\frac{m_\Lambda|\vec{p}_D|}{|\vec{k}|W} \tag{11}$$

with the fine-structure constant $\alpha \sim 1/137$.

A. The Regge model

The Regge model provides us with an economical (fewer coupling constants needed to introduce) and elegant way to describe the photoproduction of mesons at high energies. Recently, this kind of approach has been quite successfully used to describe, with addition of several nucleon resonances in the s-channel, the photoproduction of $K^+\Lambda$ on the proton [80]. Analyticity of the scattering amplitude is built in these models. The exchange of meson trajectories (in the t channel) or baryon trajectories (in the u channel) ensures unitarity and describes the behavior of the amplitudes far from the poles. A striking feature is that these models exhibit the right energy and momentum dependence.

What is more, the Regge exchanges when extrapolated to the low-energy region provide us with smooth functions which are ideal to parametrize the background. However, one has to proceed with caution when adding the resonances to the Regge amplitude, which we do in our approach, as this can lead to double counting of the poles. The so-called duality hypothesis simply states that the sum of all contributing s-channel resonances equals the sum of all the t- and u-channel trajectory exchanges. In practice, however, one does not include all s-channel exchanges together with all the trajectory exchanges in t or u channels. The standard technique is composed of defining a limited number of dominant resonant states which replenish the phenomenological background. Nevertheless, the amount

of contributions added on top of the Regge amplitude should be limited to a strict minimum [85,99].

The amplitude for the exchange of a linear meson or baryon trajectory in the t or u channel, respectively,

$$\alpha_X(x) = \alpha_{X,0} + \alpha'_X(x - m_X^2), \tag{12}$$

where x equals t or u and m_X, $\alpha_{X,0}$, α'_X are mass, spin of the lightest particle X of the given trajectory, and the incline of the trajectory, respectively, can be written with help of the standard Feynman amplitude interchanging the Feynman propagator for the Regge one,

$$\frac{1}{x - m_X^2} \to \mathcal{P}^X_{\text{Regge}}(\alpha_X(x)). \tag{13}$$

The Regge amplitude then reads

$$\mathbb{M}_{\text{Regge}} = \beta_X \mathcal{P}^X_{\text{Regge}}(\alpha_X(x)), \tag{14}$$

where β_X is the residuum of the Feynman amplitude in the given pole, since in the vicinity of the t-channel or u-channel pole the Regge amplitude should coincide with the Feynman amplitude for the exchange of the given pole. We thus keep the vertex structure given by the Feynman diagrams, which correspond to the first materialization, i.e., the lightest particle, of the trajectory.

Generally, the Regge propagator reads

$$\mathcal{P}^{\zeta=\pm1}_{\text{Regge}}(s,x) = \left(\frac{s}{s_0}\right)^{\alpha_X(x)} \frac{\pi\alpha'}{\sin[\pi\alpha_X(x)]} \frac{1+\zeta e^{-i\pi\alpha_X(x)}}{2} \times \frac{1}{\Gamma[\alpha_X(x)+1]}, \tag{15}$$

where the exponential scale factor reduces the Regge contribution for $s > s_0$ for negative physical values of t. The scale parameter s_0 is chosen as $s_0 = 1$ GeV^2.

When we derive the Regge propagator, we have to differentiate between two signature parts of the trajectories, $\zeta = \pm 1$, in order to obey the convergence criteria: $\zeta = +1$ corresponds with the even and $\zeta = -1$ with the odd partial waves. Therefore, we have to sum over this factor in the propagator. Unfortunately, the theory does not allow us to determine the relative sign between the even and odd parts of the trajectory. We, therefore, end up either with a so-called constant phase, identical to 1, or a rotating phase which gives rise to a complex factor of $\exp(-i\pi\alpha(x))$. In studies of the K^+ photoproduction, the rotating phase has been preferred because the constant phase inducing a real amplitude leads to the hyperon polarization asymmetry being zero, which disagrees with the experimental data [85,99]. The rotating phase in the K^+ photoproduction was also derived in Refs. [100,101], where the duality diagram in the K^+ photoproduction was introduced by assuming the vector meson dominance. As the contributions of the meson and Λ_c^+ exchanges are rather weak in $\bar{D}^0\Lambda_c^+$ photoproduction, the choice of constant or rotating phase is not decisive for the background shape. In this work, we use the rotating phase of the propagator, once the experimental data on the charmed-baryon polarization asymmetry in the $\bar{D}^0$ photoproduction become available, we can check if our choice of the rotating phase in the propagator agrees with observations.

1. $\bar{D}^0$-meson trajectory exchange in the t channel

In case of the $\bar{D}^0(1864)$ pseudoscalar meson being exchanged in the t channel, shown in Fig. 1(b), the amplitude has the form

$$\mathbb{M}_{\bar{D}^0} = \bar{u}(p_\Lambda) V_S f_t(t) \frac{1}{t - m_D^2} V_\mu^{\text{EM}} \varepsilon^\mu(k) u(p), \tag{16}$$

where $f_t(t)$ is the hadron form factor and V_S is the strong vertex factor. In the strong vertex, we can consider either a pseudoscalar coupling or a pseudovector one; for corresponding vertex factor formulas, see Eqs. (22) and (23). The electromagnetic vertex factor V_μ^{EM} reads

$$V_\mu^{\text{EM}} = -iC^{(\text{model})}(2p_D - k)_\mu, \tag{17}$$

where the $C^{(\text{model})}$ is a constant which reflects what model we use to describe the $\gamma\bar{D}^0 D^0$ vertex. Derivation of this vertex factor is given in Appendix A. This amplitude in the compact form, Eq. (4), reads

$$\mathbb{M}_{\bar{D}^0} = \bar{u}(p_\Lambda)\gamma_5 f_t(t)\left[\mathcal{A}_2\mathcal{M}_2 + \mathcal{A}_3\mathcal{M}_3 - C^{(\text{model})} g_{D\Lambda_c^+ N} \frac{k\cdot\varepsilon}{k^2}\right] u(p). \tag{18}$$

There are only two nonzero scalar amplitudes for both pseudoscalar and pseudovector cases,

$$\mathcal{A}_2 = -\mathcal{A}_3 = 2C^{(\text{model})} \frac{g_{D\Lambda_c^+ N}}{t - m_D^2}, \tag{19}$$

and the third term in Eq. (18) is the term which breaks the gauge invariance. We deal with this issue in Sec. II B.

In our analysis of $\bar{D}^0\Lambda_c^+$ photoproduction, we identify the $\bar{D}^0(1864)$ pseudoscalar-meson trajectory as the dominant contribution to the high-energy amplitude. We have also considered introducing the $D^*(2007)$ vector-meson trajectory but soon we revealed that its contribution was negligible and we, thus, decided to omit it. The corresponding propagator for the $\bar{D}^0(1864)$ trajectory has the following form:

$$\mathcal{P}^{D(1864)}_{\text{Regge}}(s,t) = \frac{(s/s_0)^{\alpha_D(t)}}{\sin[\pi\alpha_D(t)]}\frac{\pi\alpha'_D}{\Gamma[1+\alpha_D(t)]} \times \exp[-i\pi\alpha_D(t)]. \quad (20)$$

The interpretation of the Regge propagator effectively incorporating the exchange of all members of an $\alpha_D(t)$ trajectory can be easily seen from the definition of the propagator. There are poles at non negative integer values of $\alpha_D(t)$, which correspond to the zeroes of the sine function but which are not compensated by the poles of the Γ function. In the physical region of the process under study (with $t < 0$), these poles cannot be reached.

The trajectory equation for the $\bar{D}^0(1864)$ pseudoscalar meson reads

$$\alpha_D(t) = 0.73(t - m_D^2). \quad (21)$$

2. Λ_c^+-baryon trajectory exchange in the u channel

In the case a Λ_c^+ baryon is being exchanged in the u channel, shown Fig. 1(c), the strong (in the pseudoscalar and pseudovector couplings, respectively) and electromagnetic vertex factors, respectively, read

$$V_S^{\text{PS}} = g_{D\Lambda_c^+N}\gamma_5, \quad (22)$$

$$V_S^{\text{PV}} = -g'_{D\Lambda_c^+N}D^\mu\gamma_\mu\gamma_5, \quad (23)$$

$$V_\mu^{\text{EM}} = eF_1^{\Lambda_c^+}(k^2)\gamma_\mu + ie\frac{F_2^{\Lambda_c^+}(k^2)}{2m_\Lambda}\sigma_{\mu\nu}k^\nu, \quad (24)$$

where $g'_{D\Lambda_c^+N} = g_{D\Lambda_c^+N}/(m_\Lambda + m_p)$, $\sigma_{\mu\nu} = \frac{i}{2}[\gamma_\mu, \gamma_\nu]$, and D^μ is a four-momentum corresponding to the $\bar{D}^0$-meson field coming out of the strong vertex. In the s and u channels, there is $D^\mu = p_D^\mu$ while in the t channel we have $D^\mu = (p - p_\Lambda)^\mu$.

At the photoproduction point ($k^2 = 0$), the Dirac $F_1^{\Lambda_c^+}$ and Pauli form factors $F_2^{\Lambda_c^+}$ acquire values

$$F_1^{\Lambda_c^+}(0) = 1, \qquad F_2^{\Lambda_c^+}(0) = \kappa_{\Lambda_c^+}, \quad (25)$$

where $\kappa_{\Lambda_c^+}$ is the anomalous magnetic moment of the Λ_c^+ baryon. Its determination belongs to the actual topics in physics, and various models [102] give results in the range

$$\kappa_{\Lambda_c^+} = (0.34 - 0.43)\mu_N.$$

In this work, we take $\kappa_{\Lambda_c^+} = 0.4\mu_N$.

The Born u-channel amplitude reads

$$\mathbb{M}_{\Lambda_c^+} = \bar{u}(p_\Lambda)V_\mu^{\text{EM}}\frac{\not{p}_\Lambda - \not{k} + m_\Lambda}{u - m_\Lambda^2}V_S f_u(u)\epsilon^\mu(k)u(p). \quad (26)$$

It can be decomposed into electric ($\sim\gamma_\mu$) and magnetic ($\sim\sigma_{\mu\nu}k^\nu$) parts according to the terms in the electromagnetic vertex factor. Opting for the pseudoscalar coupling in the strong vertex, once we cast this amplitude into the compact form

$$\begin{aligned}\mathbb{M}^{\text{PS}}_{\Lambda_c^+} = &-\frac{eg_{D\Lambda_c^+N}}{u - m_\Lambda^2}\bar{u}(p_\Lambda)\gamma_5 f_u(u)\left[-\mathcal{M}_1 - 2\mathcal{M}_3 + (u - m_\Lambda^2)\frac{k\cdot\varepsilon}{k^2}\right]u(p) \\ &-\frac{eg_{D\Lambda_c^+N}}{u - m_\Lambda^2}\bar{u}(p_\Lambda)\gamma_5 f_u(u)\frac{\kappa_{\Lambda_c^+}}{4m_\Lambda}[-2m_\Lambda\mathcal{M}_1 - 4\mathcal{M}_5 - 2\mathcal{M}_6]u(p), \end{aligned} \quad (27)$$

we recognize the scalar amplitudes $\mathcal{A}_i, i = 1, \ldots, 6$ which read

$$\mathcal{A}_1 = \frac{eg_{D\Lambda_c^+N}}{u - m^2_{\Lambda_c^+}}f_u(u)\left[1 + \frac{\kappa_{\Lambda_c^+}}{2}\right], \quad (28a)$$

$$\mathcal{A}_3 = 2\frac{eg_{D\Lambda_c^+N}}{u - m^2_{\Lambda_c^+}}f_u(u), \quad (28b)$$

$$\mathcal{A}_5 = \frac{eg_{D\Lambda_c^+N}}{u - m^2_{\Lambda_c^+}}f_u(u)\frac{\kappa_{\Lambda_c^+}}{m_\Lambda} = 2\mathcal{A}_6. \quad (28c)$$

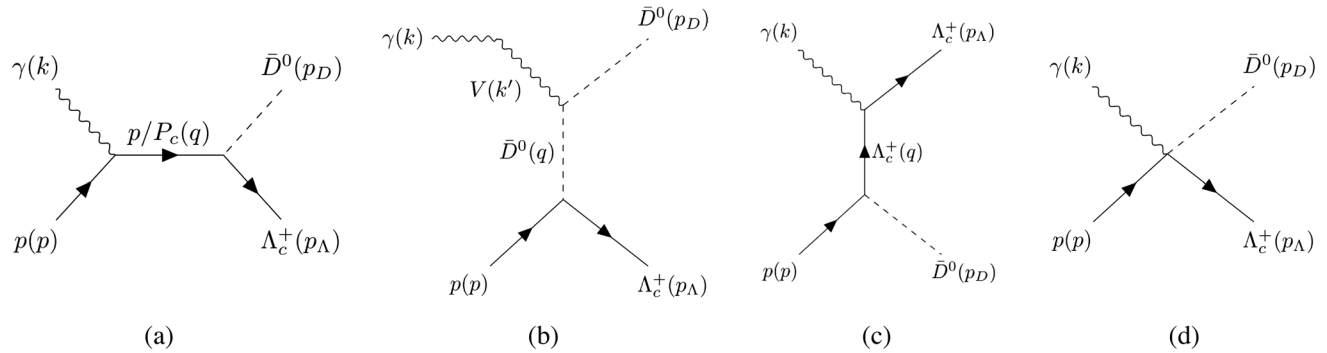

FIG. 1. Feynman diagrams of the contributions to the $p(\gamma, \bar{D}^0)\Lambda_c^+$. The background part is modeled by assuming either the exchange of a $\bar{D}^0$-meson trajectory in the t channel, where the photon couples to the $\bar{D}^0$-meson with help of intermediary vector meson (b), or a Λ_c^+-baryon trajectory in the u channel (c). In order to restore the gauge invariance, we add the contact term (d) and the proton exchange (a). On top of the background, there are s-channel exchanges of pentaquarks (a).

When we use the pseudovector coupling in the strong vertex, the invariant amplitude, split into the electric and magnetic terms, reads

$$\begin{aligned}\mathbb{M}^{\mathrm{PV}}_{\Lambda_c^+} = &-\frac{e g'_{D\Lambda_c^+ N}}{u-m_\Lambda^2}\bar{u}(p_\Lambda)\gamma_5 f_u(u)\Big[-(m_\Lambda+m_p)\mathcal{M}_1 \\ &-2(m_\Lambda+m_p)\mathcal{M}_3+\left(2\frac{k\cdot p_\Lambda}{k^2}-1\right)\mathcal{M}_6+(u-m_\Lambda^2)\frac{k\cdot\varepsilon}{k^2}(m_p+m_\Lambda+\not{k})\Big]u(p) \\ &+\frac{e g'_{D\Lambda_c^+ N}}{u-m_\Lambda^2}\bar{u}(p_\Lambda)\gamma_5 f_u(u)\frac{\kappa_{\Lambda_c^+}}{4m_\Lambda}[(u-m_\Lambda^2+4m_\Lambda m_p)\mathcal{M}_1+4(m_\Lambda+m_p)\mathcal{M}_5+2(m_\Lambda+m_p)\mathcal{M}_6]u(p). \quad (29)\end{aligned}$$

The extracted scalar amplitudes have the form

$$\mathcal{A}_1 = \frac{e g'_{D\Lambda_c^+ N}}{u-m_\Lambda^2} f_u(u)\left[m_\Lambda+m_p+\frac{\kappa_{\Lambda_c^+}}{4m_\Lambda}(u-m_\Lambda^2+4m_\Lambda m_p)\right], \quad (30a)$$

$$\mathcal{A}_3 = 2\frac{e g_{D\Lambda_c^+ N}}{u-m_\Lambda^2} f_u(u), \quad (30b)$$

$$\mathcal{A}_5 = \frac{e g_{D\Lambda_c^+ N}}{u-m_\Lambda^2} f_u(u)\frac{\kappa_{\Lambda_c^+}}{m_\Lambda}, \quad (30c)$$

$$\mathcal{A}_6 = \frac{e g_{D\Lambda_c^+ N}}{u-m_\Lambda^2} f_u(u)\left[\frac{1}{m_\Lambda+m_p}\left(1-2\frac{k\cdot p_\Lambda}{k^2}\right)+\frac{\kappa_{\Lambda_c^+}}{2m_\Lambda}\right]. \quad (30d)$$

Moreover, we can clearly see the gauge breaking term, $\sim k\cdot\varepsilon/k^2$, in the electric part of the amplitude. This term, however, needs to be canceled in the total amplitude, which is done with help of the s-channel proton exchange and the contact current.

Since the first materialization of the Λ_c^+ trajectory carries spin, $\alpha_{X,0}$ in Eq. (12) takes on the value of the spin. In this case, thus $\alpha_{X,0}=1/2$. The trajectory equation for the Λ_c^+ baryon reads

$$\alpha_\Lambda(u) = 0.5 + 0.65(u-m_\Lambda^2). \quad (31)$$

The effect of spin can be implemented into the Regge propagator, Eq. (15), in a simple way by making the replacement $\alpha_X \to \alpha_X - \alpha_{X,0}$. This substitution guarantees that the Regge amplitude matches the corresponding Feynman one at the pole of the first materialization where $\alpha_X = \alpha_{X,0}$. The corresponding propagator for the $\Lambda_c^+(2286)$ trajectory has the following form:

$$\mathcal{P}^{\Lambda_c^+(2286)}_{\mathrm{Regge}}(s,u) = \frac{(s/s_0)^{\alpha_\Lambda(u)-1/2}}{\sin[\pi(\alpha_\Lambda(u)-1/2)]}\frac{\pi\alpha'_\Lambda}{\Gamma[1/2+\alpha_\Lambda(u)]} \times \exp[-i\pi(\alpha_\Lambda(u)-1/2)]. \quad (32)$$

B. Gauge-invariance restoration

The gauge invariance or electromagnetic current conservation is a fundamental requirement which any physical theory should fulfil. In the process under study in this paper, the pseudoscalar-meson exchange in the t channel and the Λ_c^+-baryon exchange in the u channel explicitly break the gauge invariance [see Eqs. (18), (27), and (29)].

There are generally two methods to restore gauge invariance. A very often used prescription for the gauge-invariance restoration in the Regge model is the Guidal-Laget-Vanderhaeghen method [103]. In this method, in order to restore the gauge invariance broken by the t-channel exchange, the authors add the electric part of the s-channel Born diagram to the t-channel exchanges of the Regge trajectories. The gauge noninvariant terms coming from both s-channel and t-channel diagrams then compensate each other so that the total amplitude becomes gauge invariant. Although this framework provides a reliable data description, recent criticism revealed that it is not substantiated in any approximation of the field theory [104]. An introduction of the contact term in order to tame the gauge noninvariant contributions of the t channel meson-trajectory exchange was proposed [104]. We follow this prescription and introduce the contact term in both t-channel and u-channel trajectory exchanges. What is more, in order to cancel the gauge breaking terms coming from the u-channel exchanges, we need to introduce also the s-channel proton exchange.

1. $\bar{D}^0$-meson trajectory exchange in the t channel

When we consider the Reggeization of the t-channel exchanges of the $\bar{D}^0$-meson trajectory, we have to introduce a contact term in order to tame the gauge noninvariant contributions stemming from the t-channel amplitude. The contact term has to fulfil the four-divergence condition [104],

$$k_\mu \mathbb{M}^\mu_{\mathrm{int}} = Q_D F_t + Q_{\Lambda_c^+} F_u - F_s Q_p, \quad (33)$$

where $Q_D = C^{(\mathrm{model})}$ is a constant associated to the strength of the γDD effective Lagrangian (see Appendix A for more details), $Q_{\Lambda_c^+} = Q_p = e$ are charges associated to the Λ_c^+

baryon and proton, respectively, and $F_x, x = s, t, u$, denote the vertex factors in the s, t, and u channels, respectively.

The minimal contact term reads

$$\mathbb{M}^{\mu}_{\text{int}} = m^{\mu}_c f_t(t) + V_S C^{\mu}, \tag{34}$$

where the first term is the so-called Kroll-Ruderman–type bare contact current m^{μ}_c resulting from an elementary four-point Lagrangian multiplied by the hadron form factor in the t channel, and the other term is an auxiliary current C^{μ} multiplied by the strong vertex factor V_S. When we put all hadron form factors to unity, the contact term is determined by the first term only, i.e., $\mathbb{M}^{\mu}_{\text{int}} = m^{\mu}_c$. Inserting the above mentioned values for Q's and the pseudoscalar coupling in the strong vertex, when $F_t = F_u = F_s = g_{D\Lambda_c^+ N}\gamma_5$, into the four-divergence condition, Eq. (33), we get

$$k_\mu \mathbb{M}^{\mu}_{\text{int}} = k_\mu m^{\mu}_c = C^{(\text{model})} g_{D\Lambda_c^+ N}\gamma_5 \frac{k^\mu k_\mu}{k^2}. \tag{35}$$

Contracting m^{μ}_c with the photon polarization vector $\varepsilon_\mu(k)$ and introducing the hadron form factor $f_t(t)$ gives us precisely the term which we need to cancel the gauge-violating term in the t-channel amplitude, Eq. (18), i.e.,

$$m^{\mu}_c \varepsilon_\mu(k) f_t(t) = C^{(\text{model})} g_{D\Lambda_c^+ N} f_t(t)\gamma_5 \frac{k\cdot\varepsilon}{k^2}. \tag{36}$$

When we opt for the pseudovector coupling in the strong vertex, we can proceed in a completely analogous way. We just need to keep in mind that the strong vertex coupling in this case varies in various channels as it involves the four-momentum of a $\bar{D}^0$-meson field going out of the strong vertex; see Eq. (23). Therefore, $F_t = -g'_{D\Lambda_c^+ N}(\not{p} - \not{p}_\Lambda)\gamma_5$ and $F_u = F_s = -g'_{D\Lambda_c^+ N}\not{p}_D\gamma_5$, where $g'_{D\Lambda_c^+ N} = g_{D\Lambda_c^+ N}/(m_\Lambda + m_p)$. The contraction of m^{μ}_c with the photon polarization vector $\varepsilon_\mu(k)$ multiplied by the hadron form factor $f_t(t)$ gives

$$m^{\mu}_c \varepsilon_\mu(k) f_t(t) = -C^{(\text{model})} g'_{D\Lambda_c^+ N} f_t(t)(\not{p} - \not{p}_\Lambda)\gamma_5 \frac{k\cdot\varepsilon}{k^2}. \tag{37}$$

Once we sandwich this expression by the Dirac bispinors of the Λ_c^+ and proton from the left and right, respectively, and employ the Dirac equation, we end up with the same expression that we encountered in the case with the pseudoscalar coupling, i.e., Eq. (36).

Using only the first term in the minimal contact current, Eq. (34), is thus sufficient to restore the gauge invariance of the amplitude. Interestingly, the contact term serves only to cancel the gauge-violating term in Eq. (18) and it does not contribute to scalar amplitudes $\mathcal{A}_j$.

2. Λ_c^+-baryon trajectory exchange in the u channel

In case we consider the Reggeization of the u-channel Λ_c^+ exchanges, the total amplitude reads

$$\mathbb{M}^{\mu} = \mathbb{M}^{\mu}_s + \mathbb{M}^{\mu}_u + \mathbb{M}^{\mu}_{\text{int}}, \tag{38}$$

where $\mathbb{M}^{\mu}_x$ is the amplitude of either an s-channel ($x = s$) or a u-channel ($x = u$) exchange and $\mathbb{M}^{\mu}_{\text{int}}$ is the contact current which can be written in the form

$$\mathbb{M}^{\mu}_{\text{int}} = m^{\mu}_c f_u(u) + V_S C^{\mu}. \tag{39}$$

When we consider the Λ_c^+-baryon trajectory exchange in the u channel and do not assume the vector meson dominance in the t channel [in which case $Q_D = 0$ in Eq. (33)], the gauge-violating terms come only from the u and s channels. The Kroll-Ruderman–type bare contact current m^{μ}_c therefore needs to satisfy the condition

$$k_\mu m^{\mu}_c = Q_{\Lambda_c^+} F_u - F_s Q_p. \tag{40}$$

The four-divergence vanishes since $Q_{\Lambda_c^+} = Q_p = e$ and both u-channel and s-channel vertex factors coincide, i.e., $F_u = F_s = V_S^{\text{PS}}$, in the pseudoscalar coupling. Therefore, $m^{\mu}_c = 0$. The contact current is thus determined by the second term in Eq. (39) only. The auxiliary current C^{μ} is given by

$$C^{\mu} = -e\left[(2p_\Lambda - k)^\mu \frac{f_u - 1}{u - m_\Lambda^2} f_s + (2p + k)^\mu \frac{f_s - 1}{s - m_p^2} f_u\right]. \tag{41}$$

With help of this knowledge on the shape of the contact current, we can recast it into the compact form in order to extract its contributions. When we employ the pseudoscalar coupling in the strong vertex, we get

$$\begin{aligned}\mathbb{M}^{\text{PS}}_{\text{int}} &= \bar{u}(p_\Lambda) V_S^{\text{PS}} C^\mu \varepsilon_\mu(k) u(p) \\ &= -e g_{D\Lambda_c^+ N}\bar{u}(p_\Lambda)\gamma_5 \Bigg\{\left[2\mathcal{M}_3 - (u - m_\Lambda^2)\frac{k\cdot\varepsilon}{k^2}\right] \\ &\quad \times \frac{f_u(u) - 1}{u - m_\Lambda^2} f_s(s) \\ &\quad + \left[2\mathcal{M}_2 + (s - m_p^2)\frac{k\cdot\varepsilon}{k^2}\right]\frac{f_s(s) - 1}{s - m_p^2} f_u(u)\Bigg\} u(p).\end{aligned} \tag{42}$$

The contact term contributions to the scalar amplitudes read

$$\mathcal{A}_2 = -2e g_{D\Lambda_c^+ N}\frac{f_s(s) - 1}{s - m_p^2} f_u(u), \tag{43a}$$

$$\mathcal{A}_3 = -2e g_{D\Lambda_c^+ N}\frac{f_u(u) - 1}{u - m_\Lambda^2} f_s(s). \tag{43b}$$

It can be easily shown that the Kroll-Ruderman bare contact current m_c^μ vanishes also with the pseudovector coupling. It is sufficient to realize that the pseudovector strong vertex factors F_u and F_s in Eq. (40) coincide, i.e., $F_u = F_s = -g'_{D\Lambda_c^+N}\not{p}_D\gamma_5$, as well as the charges associated to the Λ_c^+ baryon and proton, $Q_{\Lambda_c^+} = Q_p = e$, respectively.

The contact current contribution is thus given solely by the auxiliary current C^μ and reads

$$\begin{aligned}\mathbb{M}_{\rm int}^{\rm PV} &= \bar{u}(p_\Lambda)V_S^{\rm PV}C^\mu\varepsilon_\mu(k)u(p)\\ &= \bar{u}(p_\Lambda)V_S^{\rm PS}C^\mu\varepsilon_\mu(k)u(p)\\ &\quad - eg'_{D\Lambda_c^+N}\bar{u}(p_\Lambda)\gamma_5\not{k}\left\{[2p_\Lambda\cdot\varepsilon - k\cdot\varepsilon]\frac{f_u-1}{u-m_\Lambda^2}f_s + [2p\cdot\varepsilon + k\cdot\varepsilon]\frac{f_s-1}{s-m_p^2}f_u\right\}u(p)\\ &= -eg'_{D\Lambda_c^+N}\bar{u}(p_\Lambda)\gamma_5\left\{\left[2(m_\Lambda+m_p)\mathcal{M}_3 - 2\mathcal{M}_5 + \left(1-\frac{k\cdot p_\Lambda}{k^2}\right)\mathcal{M}_6 - (u-m_\Lambda^2)(m_\Lambda+m_p+\not{k})\frac{k\cdot\varepsilon}{k^2}\right]\frac{f_u-1}{u-m_\Lambda^2}f_s\right.\\ &\quad \left. + \left[2(m_\Lambda+m_p)\mathcal{M}_2 - 2\mathcal{M}_4 - 2\frac{k\cdot p}{k^2}\mathcal{M}_6 + (s-m_p^2)(m_\Lambda+m_p+\not{k})\frac{k\cdot\varepsilon}{k^2}\right]\frac{f_s-1}{s-m_p^2}f_u\right\}u(p). \end{aligned} \tag{44}$$

In the pseudovector coupling, the contact term contributions, beyond the contributions of Eq. (43), read

$$\mathcal{A}_4 = 2eg'_{D\Lambda_c^+N}\frac{f_s-1}{s-m_p^2}f_u, \tag{45a}$$

$$\mathcal{A}_5 = 2eg'_{D\Lambda_c^+N}\frac{f_u-1}{u-m_\Lambda^2}f_s, \tag{45b}$$

$$\mathcal{A}_6 = eg'_{D\Lambda_c^+N}\left[2\frac{k\cdot p}{k^2}\frac{f_s-1}{s-m_p^2}f_u - \left(1-\frac{k\cdot p_\Lambda}{k^2}\right)\frac{f_u-1}{u-m_\Lambda^2}f_s\right]. \tag{45c}$$

The Reggeization of the u-channel and contact-current contributions corresponds to substituting the Regge rezidual function $\mathcal{F}_u(u) = (u-m_\Lambda^2)\mathcal{P}_{\rm Regge}^\Lambda$ for the usual hadron form factor $f_u(u)$ in all the expressions above.

In order to restore the gauge invariance in the u channel, we add not only the contact current but also a proton exchange in the s channel. The strong vertex functions are the same as shown above in Eqs. (22) and (23) and the electromagnetic vertex function reads

$$V_\mu^{\rm EM} = eF_1^p(k^2)\gamma_\mu + e\frac{1-F_1^p(k^2)}{k^2}k_\mu\gamma\cdot k + ie\frac{F_2^p(k^2)}{2m_p}\sigma_{\mu\nu}k^\nu, \tag{46}$$

where $F_1^p(k^2)$ and $F_2^p(k^2)$ are standard electromagnetic proton form factors for which at the photoproduction point holds $F_1^p(0) = 1$ and $F_2^p(0) = \kappa_p$, where κ_p is the anomalous proton magnetic moment.

The invariant amplitude of the proton exchange reads

$$\mathbb{M}_p = \bar{u}(p_\Lambda)V_S f_s(s)\frac{\not{p}+\not{k}+m_p}{s-m_p^2}V_\mu^{\rm EM}\varepsilon^\mu(k)u(p) \tag{47}$$

and, similarly to the u-channel case, it can be divided into the electric and magnetic parts, each corresponding to the appropriate term in the electromagnetic vertex factor. We choose the pseudoscalar coupling in the strong vertex and cast the amplitude into the compact form,

$$\begin{aligned}\mathbb{M}_p^{\rm PS} &= \frac{eg_{D\Lambda_c^+N}}{s-m_p^2}\bar{u}(p_\Lambda)\gamma_5 f_s(s)\left[\mathcal{M}_1 + 2\mathcal{M}_2\right.\\ &\quad \left. + (s-m_p^2)\frac{k\cdot\varepsilon}{k^2}\right]u(p)\\ &\quad - \frac{eg_{D\Lambda_c^+N}}{s-m_p^2}\bar{u}(p_\Lambda)\gamma_5 f_s(s)\frac{\kappa_p}{4m_p}[-4m_p\mathcal{M}_1\\ &\quad - 4\mathcal{M}_4 + 2\mathcal{M}_6]u(p). \end{aligned} \tag{48}$$

We can then extract the scalar amplitudes

$$\mathcal{A}_1 = \frac{eg_{D\Lambda_c^+N}}{s-m_p^2}f_s(s)[1+\kappa_p], \tag{49a}$$

$$\mathcal{A}_2 = 2\frac{eg_{D\Lambda_c^+N}}{s-m_p^2}f_s(s), \tag{49b}$$

$$\mathcal{A}_4 = \frac{eg_{D\Lambda_c^+N}}{s-m_p^2}f_s(s)\frac{\kappa_p}{m_p} = -2\mathcal{A}_6. \tag{49c}$$

When we use the pseudovector coupling in the strong vertex, the amplitude takes the form

$$\mathbb{M}_p^{\mathrm{PV}} = \bar{u}(p_\Lambda)\gamma_5 \frac{e g'_{D\Lambda_c^+ N}}{s-m_p^2} f_s(s) \Big[(m_\Lambda + m_p)(\mathcal{M}_1 + 2\mathcal{M}_2) - (1 + 2k\cdot p/k^2)\mathcal{M}_6 + (s-m_p^2)(m_\Lambda + m_p + \not{k})\frac{k\cdot\varepsilon}{k^2}\Big] u(p) + \bar{u}(p_\Lambda)\gamma_5 \frac{e g'_{D\Lambda_c^+ N}}{s-m_p^2} f_s(s) \frac{\kappa_p}{2m_p} \{[2k\cdot p + k^2]\mathcal{M}_1 + 2(m_\Lambda + m_p)\mathcal{M}_4 - (m_\Lambda + m_p)\mathcal{M}_6\} u(p), \quad (50)$$

where $g'_{D\Lambda_c^+ N} = g_{D\Lambda_c^+ N}/(m_\Lambda + m_p)$.

The scalar amplitudes read

$$\mathcal{A}_1 = \frac{e g_{D\Lambda_c^+ N}}{s-m_p^2} f_s(s) \left[1 + \frac{\kappa_p}{2m_p(m_\Lambda + m_p)}(s-m_p^2)\right], \quad (51a)$$

$$\mathcal{A}_2 = 2\frac{e g_{D\Lambda_c^+ N}}{s-m_p^2} f_s(s), \quad (51b)$$

$$\mathcal{A}_4 = \frac{e g_{D\Lambda_c^+ N}}{s-m_p^2} f_s(s) \frac{\kappa_p}{m_p}, \quad (51c)$$

$$\mathcal{A}_6 = -\frac{e g_{D\Lambda_c^+ N}}{s-m_p^2} f_s(s) \left[\frac{1}{m_\Lambda + m_p}\left(1 + 2\frac{k\cdot p}{k^2}\right) + \frac{\kappa_p}{2m_p}\right]. \quad (51d)$$

In both pseudoscalar and pseudovector cases, the gauge-breaking terms come from the electric part of the interaction, while the magnetic part is gauge invariant.

From this treatise, we can clearly see that the gauge-breaking terms in both s and u channels are wiped out and the total amplitude is gauge invariant.

C. Pentaquark exchanges

On top of the Regge background, we add the pentaquark exchanges in the s channel, as shown in Fig. 1(a), with the standard Feynman propagators and the resonance finite lifetime which is taken into account through the substitution

$$s - m_{P_c}^2 \to s - m_{P_c}^2 + i m_{P_c}\Gamma_{P_c}$$

in the propagator denominator where the m_{P_c} and Γ_{P_c} are the mass and width of the propagating pentaquark state, respectively. There are three pentaquark states that we take into account, two with spin $1/2$ and one with spin $3/2$. Table I summarizes their properties.

1. Spin-1/2 pentaquark exchange

The amplitude for this contribution has the form

$$\mathbb{M}_{P_c(1/2)} = \mathrm{i}\bar{u}(p_\Lambda) g_{D\Lambda_c P_c}\gamma_5\Gamma f_s(s) \frac{\not{q} + m_{P_c}}{s - m_{P_c}^2 + \mathrm{i} m_{P_c}\Gamma_{P_c}} \times \frac{\mu_{pP_c}}{m_p + m_{P_c}} \sigma^{\mu\nu} k_\nu \Gamma \varepsilon_\mu(k) u(p), \quad (52)$$

where μ_{pP_c} is a transition magnetic moment [97]. As both spin-1/2 pentaquark states are of negative parity, the factor Γ takes the form of γ_5. In this case, the scalar amplitudes are

$$\mathcal{A}_1 = \frac{m_{P_c} - m_p}{s - m_{P_c}^2 + \mathrm{i} m_{P_c}\Gamma_{P_c}} G, \quad (53a)$$

$$\mathcal{A}_4 = -\frac{2}{s - m_{P_c}^2 + \mathrm{i} m_{P_c}\Gamma_{P_c}} G, \quad (53b)$$

$$\mathcal{A}_6 = -\frac{1}{2}\mathcal{A}_4, \quad (53c)$$

where

$$G = g_{D\Lambda_c P_c}\frac{\mu_{pP_c}}{m_p + m_{P_c}} \quad (54)$$

is the coupling parameter.

2. Spin-3/2 pentaquark exchange

The amplitude of the spin-3/2 pentaquark exchange reads

$$\mathbb{M}_{P_c(3/2)} = \bar{u}(p_\Lambda)\Gamma \frac{\mathrm{i} f}{m_{P_c} m_D} \epsilon_{\mu\nu\lambda\rho}\gamma_5\gamma^\lambda q^\mu p_D'^\rho f_s(s) \times \frac{\not{q} + m_{P_c}}{s - m_{P_c}^2 + \mathrm{i} m_{P_c}\Gamma_{P_c}} \left(g^{\nu\beta} - \frac{1}{3}\gamma^\nu\gamma^\beta\right) \times \frac{1}{m_{P_c}(m_{P_c} + m_p)} (g_1 q^\alpha F_{\alpha\beta} + g_2 \not{q} F_{\beta\alpha}\gamma^\alpha - g_2\gamma_\beta q^\alpha F_{\alpha\tau}\gamma^\tau)\Gamma\gamma_5 u(p), \quad (55)$$

where $F_{\mu\nu} = k_\mu\varepsilon_\nu - \varepsilon_\mu k_\nu$, g_1 and g_2 are the electromagnetic coupling constants, and f is the strong coupling constant. As the $P_c(4440)$ pentaquark has negative parity, the factor Γ equals γ_5. Casting the amplitude to the compact form (4), the extracted individual scalar amplitudes $\mathcal{A}_j$ read

$$\mathcal{A}_1' = -\frac{G_1}{3}(q\cdot p_\Lambda - m_{P_c} m_\Lambda) q\cdot k + \frac{G_2}{3}(2s q\cdot p_\Lambda - 3s k\cdot p_\Lambda + 2s m_p m_\Lambda + m_{P_c} m_\Lambda q\cdot k - 2s m_{P_c} m_\Lambda - 2m_p m_{P_c} q\cdot p_\Lambda + 2q\cdot p_\Lambda q\cdot k), \quad (56a)$$

$$\mathcal{A}_2' = G_1\left[sk\cdot p_\Lambda + m_{P_c}m_p k\cdot p_\Lambda - \frac{1}{3}q\cdot p_\Lambda k^2 + \frac{1}{3}m_{P_c}m_\Lambda k^2\right] + G_2\left[-2sk\cdot p_\Lambda + \frac{1}{3}m_\Lambda m_{P_c}k^2 + \frac{2}{3}k^2 q\cdot p_\Lambda\right], \quad (56b)$$

$$\mathcal{A}_3' = G_1(-m_{P_c}m_p - s)q\cdot k + G_2(2q\cdot k - k^2)s, \quad (56c)$$

$$\mathcal{A}_4' = G_1\left[-\frac{1}{3}sm_\Lambda + \frac{1}{3}(m_p + m_{P_c})q\cdot p_\Lambda - \frac{1}{3}m_\Lambda m_p m_{P_c} - m_{P_c}k\cdot p_\Lambda\right] - G_2\left[-sm_\Lambda + \frac{1}{3}m_\Lambda m_p m_{P_c} + \frac{2}{3}m_p q\cdot p_\Lambda\right], \quad (56d)$$

$$\mathcal{A}_5' = G_1 m_{P_c}q\cdot k + G_2(-m_{P_c} + m_p)s, \quad (56e)$$

$$\mathcal{A}_6' = G_1\left[\frac{1}{3}m_\Lambda m_p m_{P_c} + m_{P_c}k\cdot p_\Lambda + \frac{1}{3}m_\Lambda s - \frac{1}{3}q\cdot p_\Lambda(m_p + m_{P_c})\right] + G_2\left[-\frac{1}{3}m_\Lambda s + \frac{1}{3}m_\Lambda m_p m_{P_c} + \frac{2}{3}q\cdot p_\Lambda(m_p - m_{P_c})\right], \quad (56f)$$

where the coupling parameters G_1 and G_2 read

$$G_1 = -\frac{fg_1}{16m_D^4 m_p^4}, \quad (57a)$$

$$G_2 = -\frac{fg_2}{32m_D^4 m_p^5}. \quad (57b)$$

Each amplitude $\mathcal{A}_i', i = 1,\ldots,6$, has to be multiplied by the propagator denominator

$$\mathcal{A}_i = \frac{1}{s - m_{P_c}^2 + \mathrm{i}m_{P_c}\Gamma_{P_c}}\mathcal{A}_i'. \quad (58)$$

III. DISCUSSION OF RESULTS

In this section, we present our new model for the $\bar{D}^0\Lambda_c^+$ photoproduction off proton and show its predictions of the differential cross sections for energies from the threshold $E_\gamma^{\mathrm{lab}} = 8.67$ GeV up to 20 GeV. In our model, there are a few unknown parameters. Spin-1/2 and spin-3/2 pentaquark exchanges introduce one and two free parameters, respectively, and there is one more free parameter, $g_{D\Lambda_c^+N}$, which governs the trajectory behavior. For this parameter, however, we can get some hint from several distinctive approaches; either from the SU(4) symmetry, the QCD sum rules or the quark model as shown in Table II. Unfortunately, these approaches give us values which are not in accordance with each other.

Since the particles we deal with are not pointlike, we introduce also the hadron form factors, one for the background and one for the pentaquark exchanges, in order to take the extended structure of the exchanged particles into account. Each hadron form factor introduces one parameter, the cutoff parameter Λ. As there are currently no data available, we had to choose these parameters by hand. We let the values of the cutoff parameters vary from 4 to 5 GeV so as to illustrate their effects on the predictions. In other works, typical values in the $K^+\Lambda$ photoproduction are between 1 and 3 GeV, and a recent study [73] on $\bar{D}^0\Lambda_c^+$ used $\Lambda = 0.55$ GeV. Let us point out that the cutoff value depends not only on the process under study and particles involved therein but also on the choice of the hadron form factor; we know that the accurate selection of the appropriate hadron form factor is a troubling issue, e.g., in the $K^+\Lambda$ photoproduction. In a recent study of that reaction, it was revealed that the optimal hadron form factor should have the multidipole shape as it depends on the particle's spin and thus gets stronger for higher-spin particles and suppresses their contributions more. In the current study, we opt for a dipole form factor

$$F_d(\Lambda) = \frac{\Lambda^4}{(x - m^2)^2 + \Lambda^4}, \quad (59)$$

where Λ, $x = s$, t, u, and m are the cutoff parameter, the Mandelstam variable, and the mass of the exchanged particle, respectively. The reason for preferring this form factor to the other ones is that in the $\bar{D}^0\Lambda_c^+$ production we take into account only one pentaquark with spin 3/2. The remaining two pentaquarks are of spin 1/2, for which the multidipole form factor would reduce to a standard dipole one. The role of the hadron form factor lies also in suppressing contributions of the trajectories, which tend to rise with increasing energy.

In the strong vertex, we can choose between a pseudoscalar or a pseudovector coupling. This choice affects not only the shape of the cross section but also slightly changes its magnitude. The exchanges of Regge trajectories in the t or u channels produce cross sections which are smooth functions of energy. The exchange of the t-channel trajectory leads to the cross section which is focused in the forward hemisphere and peaked at around $\theta_D^{\mathrm{c.m.}} = 30°$ and which smoothly falls to zero at backward angles. The mere Regge-trajectory exchange is strongly suppressed by the factor $s^{\alpha_D(t)}$ in the Regge propagator, Eq. (20), as the Mandelstam variable t occurring in the Regge trajectory, Eq. (21), acquires large negative values (more pronounced at backward angles). In case of t-channel Reggeization, the choice of the type of coupling in the strong vertex does not affect the behavior of the contribution. We observe forward peaking of the t-channel $\bar{D}^0$-meson exchange

which acquires its maximum at around $\theta_D^{\text{c.m.}} = 20°$ and then sharply decreases with the growing angle $\theta_D^{\text{c.m.}}$. On the contrary, when we consider the u-channel trajectory with exchanges of Λ_c^+ baryons, we observe a significant change between using the pseudoscalar and pseudovector couplings and in both cases we obtain nonzero cross sections at backward angles. In case of the pseudoscalar coupling in the strong vertex, the background contribution is peaked at backward angles (see Fig. 2) while when we use the pseudovector coupling in the strong vertex, the background produces a peak at forward angles (see Fig. 3). In both cases, the u-channel trajectory exchange produces peaks at large $\theta_D^{\text{c.m.}}$ angles, but we observe a strong contribution of the proton exchange at forward angles in the pseudovector coupling which plays a decisive role in shaping the cross section. A striking feature of the u-channel background is the magnitude of its cross section prediction which is a few orders of magnitude larger in comparison with the t-channel background even though all of these contributions are calculated with the same value of the coupling constant $g_{D\Lambda_c^+N}$. The large background contribution in the u channel is caused predominantly by the contact-term and proton-exchange amplitudes. Moreover, this prediction clearly shows that we cannot omit the hadron form factor in the Reggeized u-channel background if we want to obtain reliable magnitudes of the cross section. We deal with the effect of choosing various values of the coupling constant $g_{D\Lambda_c^+N}$ on the background predictions later on.

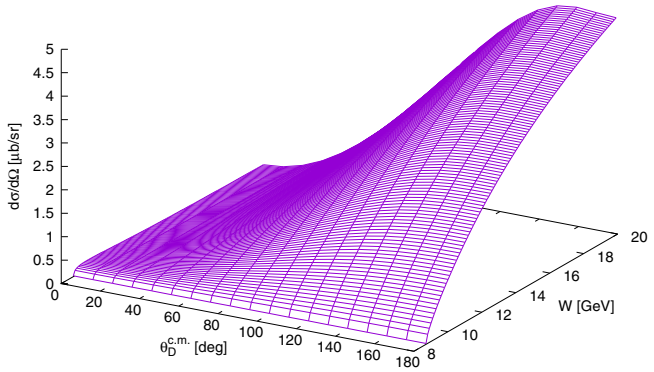

FIG. 2. Cross section as modeled by the Reggeized u-channel Λ_c^+-meson exchange with the pseudoscalar coupling in the strong vertex. Calculated with $g_{D\Lambda_c^+N}/\sqrt{4\pi} = -3.75$ and with no hadron form factor assumed.

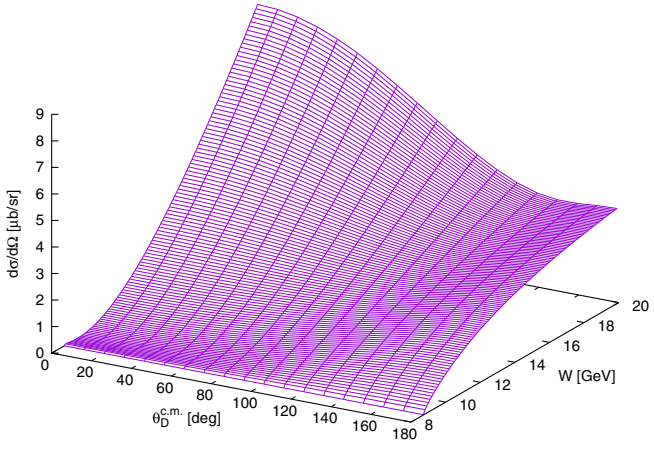

FIG. 3. Cross section as modeled by the Reggeized u-channel Λ_c^+-meson exchange with the pseudovector coupling in the strong vertex. Calculated with $g_{D\Lambda_c^+N}/\sqrt{4\pi} = -3.75$ and with no hadron form factor assumed.

The role of the contact term and the proton exchange, i.e., the terms introduced in order to cancel the gauge-breaking terms in the total amplitude, is illustrated in Fig. 4. In both pseudoscalar and pseudovector couplings, the proton exchange gives the most significant contribution, while the contact term contributes much less and affects the overall background prediction rather by interfering with the proton exchange. The role of the contact term is to mimic higher-order corrections to the tree-level description. The large contact-term contributions thus indicate a non-negligible role played by higher orders in this process. The contribution of the actual trajectory seems to be negligible, which corroborates the observation in Ref. [73] where the authors in Fig. 10 show the trajectory contributions being orders of magnitude smaller than the full model.

We also show the cross section as calculated with the full model, i.e., the three pentaquark exchanges in the s channel superimposed on the Regge background. The pentaquark

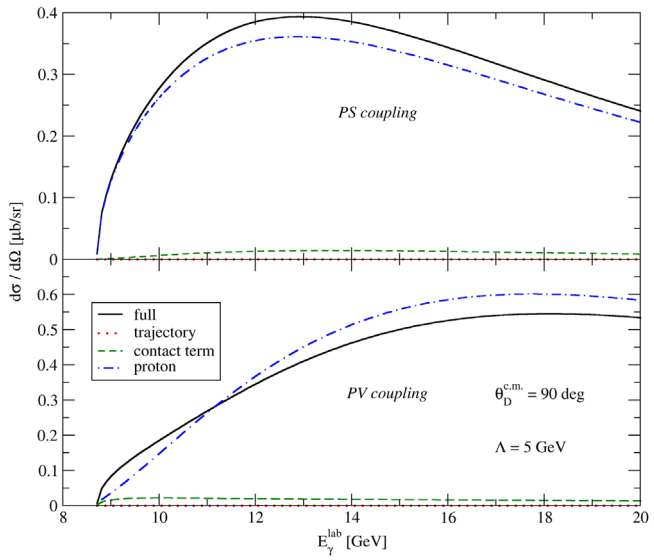

FIG. 4. The Regge background for the case of pseudoscalar (upper figure) and pseudovector (lower figure) couplings in the strong vertex. Full Regge background (solid line) and contributions of the Λ_c^+-baryon trajectory (dotted line), contact term (dashed line), and proton exchange (dotted-dashed line) are shown. Calculated for $\theta_D^{\text{c.m.}} = 90°$ and with dipole hadron form factor with cutoff parameter $\Lambda = 5$ GeV.

exchanges in the s channel produce rather sharp peaks in the cross section at the position of their poles, see Figs. 5 and 6, which show the contributions of pentaquark exchanges added on the u-channel background with the pseudoscalar and pseudovector couplings, respectively. We do not show the calculation with the Reggeized t-channel background as the background is orders of magnitude smaller than the pentaquark peaks and thus plays a very negligible role. The calculations with the Reggeized u-channel background, in both types of couplings, comprise the dipole hadron form factor with cutoff $\Lambda = 4$ GeV. In the u-channel background, the hadron form factor is indeed needed in order to suppress its large contribution. With no hadron form factor, the background contribution continues to rise with the energy. We do not, however, observe such a need in the t-channel background which contributes much less even with no hadron form factor. In this calculation, the coupling constants for the spin-1/2 and spin-3/2 pentaquarks were chosen to be 0.01 and 0.1, respectively, where

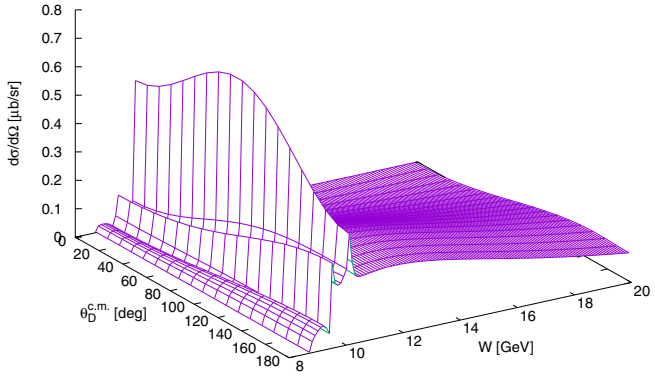

FIG. 5. Contributions of the Λ_c^+-baryon trajectory and the pentaquark exchanges in the s-channel to the cross section. The pseudoscalar coupling in the strong vertex is used. The dipole hadron form factors with $\Lambda = 4$ GeV are introduced, $g_{D\Lambda_c^+N}/\sqrt{4\pi} = -3.75$ and the couplings for spin-1/2 and spin-3/2 pentaquarks are 0.01 and 0.1, respectively.

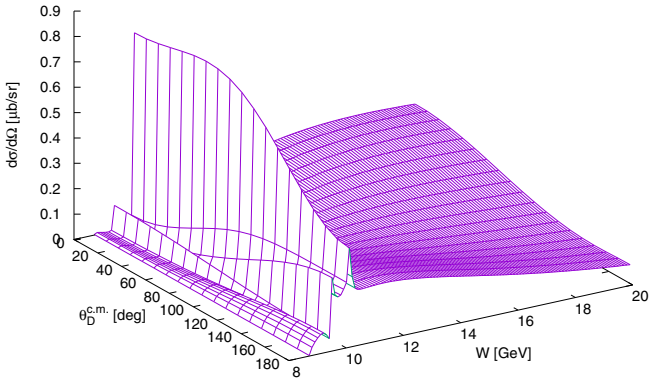

FIG. 6. Same as Fig. 5 but with the pseudovector coupling in the strong vertex.

the cross sections are obtained in a reasonable order of magnitude. We will be able to fix these coupling constants with help of partial decay widths measured in future experiments. It is also possible to predict these couplings from theoretical models. The coupling constants were not obtained in Ref. [66] referred to in this study, while we will address this calculation in future works. Interestingly, the pentaquark contributions are almost independent of the angle $\theta_D^{\text{c.m.}}$ when they are added to the t-channel background. On the other hand, we observe peaks in the central angles and in the forward angles once the pentaquark contributions interfere with the u-channel background in the pseudoscalar and pseudovector couplings, respectively.

Figure 7 shows the differential cross section in the central angles, at $\theta_D^{\text{c.m.}} = 90°$, as calculated with the t-channel $\bar{D}^0$-meson trajectory (upper figure), u-channel Λ_c^+ trajectory with the pseudoscalar (middle figure) and pseudovector (lower figure) couplings in the strong vertex. The dipole hadron form factor with the cutoff $\Lambda = 4$ GeV was introduced for both the Regge background and the pentaquark exchanges. We chose this value of the cutoff parameter since with this cutoff parameter the hadron form factor suppresses the u-channel background contributions to a reasonable level. If we do not introduce a form factor, the background contributions are an order of magnitude higher. If we do, on the other hand, employ too strong a form factor, the contributions of background almost vanish.

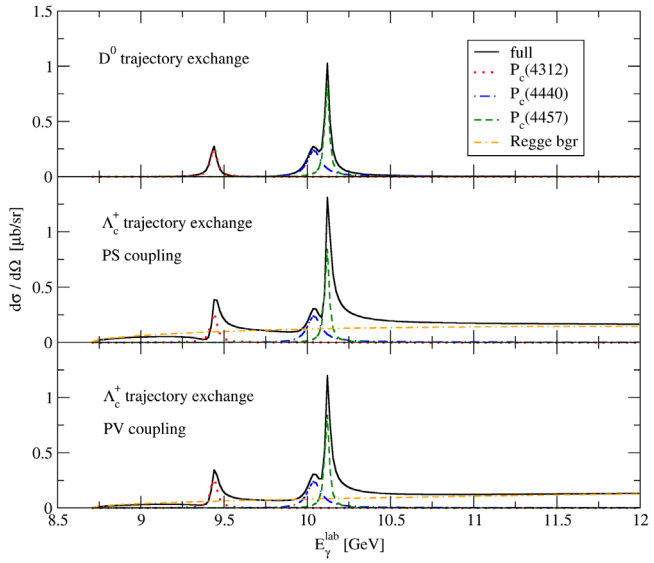

FIG. 7. Differential cross section at $\theta_D^{\text{c.m.}} = 90°$ calculated with $\bar{D}^0$-meson exchange (upper figure), Λ_c^+-baryon exchange in the pseudoscalar (middle figure) and pseudovector (lower figure) couplings in the strong vertex. The dipole hadron form factor is used with the cutoff $\Lambda = 4$ GeV. Predictions of the full model (solid line), $P_c(4312)$ only (dotted line), $P_c(4440)$ only (dashed-dotted line), $P_c(4457)$ only (dashed line), and D^0-meson trajectory only (double dashed-dotted line) are shown. The couplings are 0.01 for both $P_c(4312)$ and $P_c(4457)$ and 0.1 for $P_c(4440)$.

The differential cross section is computed with the full model, individual pentaquarks, and the Regge trajectories in either the t or u channel. We observe two narrow peaks created by the pentaquarks added on top of the smooth background created by the exchanges of the trajectories (note also the difference in the magnitudes of the t-channel and u-channel background contributions). The first peak is apparently created by the superimposition of the $P_c(4312)$ state onto the background, while the second peak is a combination of $P_c(4440)$, which creates a kind of shoulder of the actual peak, and $P_c(4457)$ contributions. The strength of the pentaquark exchange contributions depends on their couplings which unfortunately remain unknown so far. For the spin-$1/2$ pentaquarks, we opted for $G = 0.01$, while the spin-$3/2$ pentaquark couplings were chosen to be $G_1 = G_2 = 0.1$, i.e., the same values as were used above.

Figures 8 and 9 show predictions of the differential cross sections as calculated by the model with either the t-channel $\bar{D}^0$-meson exchange or the u-channel Λ_c^+-baryon exchange in the pseudoscalar and pseudovector coupling. In the case with the t-channel exchanges, we observe only two sharp peaks created by the pentaquarks and almost no background. This is in stark contrast with the case where we introduce the Reggeized u channel to model the background. In both types of coupling, we observe peaks at backward angles, mainly at and above the threshold. The Reggeized u-channel exchanges with the pseudovector coupling create also a peak at forward angles, which is more tangible at higher photon energies. The reason why the predictions of the differential cross section differ substantially for the t-channel and u-channel exchanges is obvious. In the case of the u-channel Λ_c^+-exchange, there are contributions from the Λ_c^+-exchange and on top of it there is a contribution also from the proton exchange and the contact term, both of which serve to restore the gauge invariance. The proton exchange clearly dominates and governs the shape of the background while the contact current interferes with the proton exchange and provides just minor modifications. In the case of the t-channel exchanges, there are no extra contributions for the gauge invariance preservation; the only contributions originate from the Regge trajectory which is suppressed as discussed above.

The dependence of the Regge background on the presence of the hadron form factor and values of the

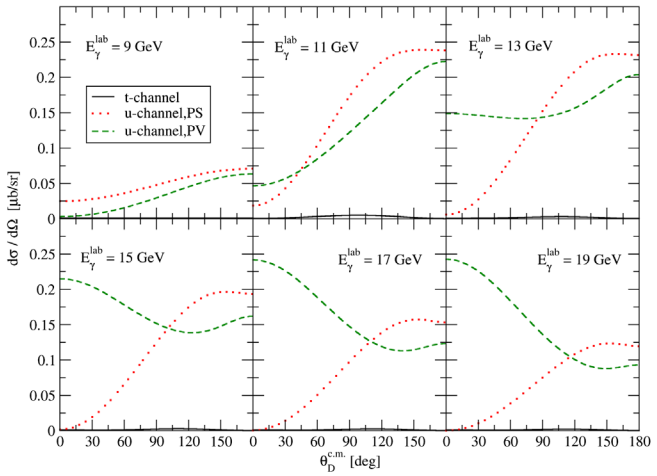

FIG. 9. Differential cross section in dependence on the $\theta_D^{\text{c.m.}}$ angle for six different photon lab energies. The background modeled by the t-channel $\bar{D}^0$-meson exchange (solid line) and u-channel Λ_c^+ exchange in the PS and PV couplings (dotted and dashed lines, respectively) is shown.

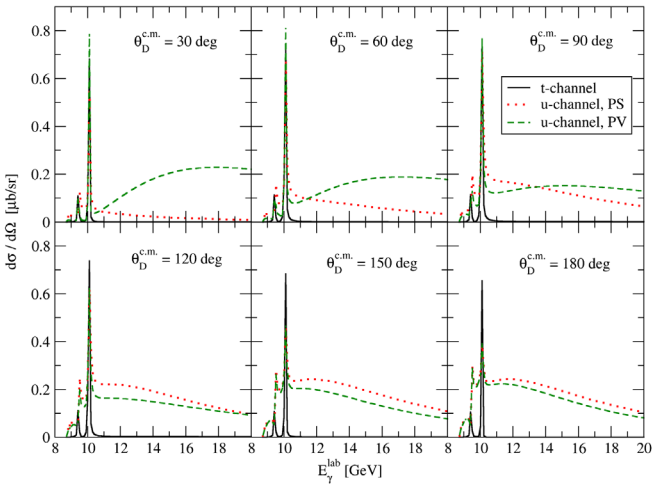

FIG. 8. Differential cross section in dependence on the photon lab energy E_γ^{lab} for six different angles. The background modeled by the t-channel $\bar{D}^0$-meson exchange (solid line) and u-channel Λ_c^+ exchange in the PS and PV couplings (dotted and dashed lines, respectively) is shown.

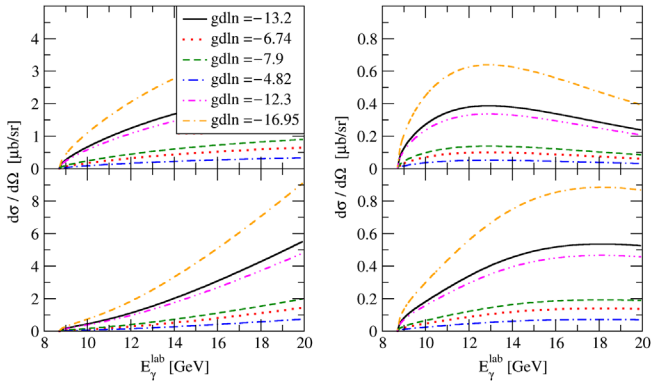

FIG. 10. Differential cross section computed for the various values of $g_{DA_c^+N}$ coupling stemming from various models as shown in Table II. Only the contribution of the Regge background is shown. The Λ_c^+-baryon exchange with the pseudoscalar (upper figure) and pseudovector (lower figure) couplings in the strong vertex is employed. The left column illustrates cases with no hadron form factor, while the right column shows suppression by the dipole hadron form factor with $\Lambda = 5$ GeV.

coupling constant $g_{D\Lambda_c^+N}$ is illustrated in Fig. 10 which collects differential cross section predictions for $\theta_D^{\mathrm{c.m.}} = 90°$ by the u-channel Regge background with either the pseudoscalar (upper row) and pseudovector (lower row) couplings in the strong vertex. In this figure, we use the $g_{D\Lambda_c^+N}$ coupling parameters from various models shown in Table II. The predictions in the left column are calculated with no hadron form factor, whereas in the right column we introduce the dipole hadron form factor with a rather large cutoff parameter $\Lambda = 5$ GeV. The overall shape of the differential cross section calculated with the u-channel Regge trajectory changes once the form factor is in use. When there is no hadron form factor, we see plateaulike and steadily rising cross sections for pseudoscalar and pseudovector couplings, respectively. However, once we employ the hadron form factor even with as large a cutoff as 5 GeV, the cross section is suppressed by an order of magnitude and its behavior changes as well. In case of the pseudoscalar coupling, we do not see the plateaulike cross section any more, for large values of $g_{D\Lambda_c^+N}$ a broad peak around $E_\gamma^{\mathrm{lab}} = 10$ GeV develops instead. Similarly, we observe a suppression of the cross section computed with the pseudovector coupling, it is most notable at higher energies where the cross section changes from a convex shape to a concave shape. The type of coupling in the strong vertex and presence of the hadron form factor thus play a decisive role in shaping the background contribution to the cross section.

IV. CONCLUSION

In this paper, we have dealt with the photoproduction of $\bar{D}^0\Lambda_c^+$ in the framework of the so-called Regge-plus-resonace model. We model the background part of the process by including an exchange of either the $\bar{D}^0$-meson trajectory in the t channel or the Λ_c^+-baryon trajectory in the u channel. In this way, we create cross sections which are smooth functions of energy. On top of this Regge background, we add exchanges of pentaquarks in the s channel which create rather sharp peaks in the cross section predictions at their respective poles. Since the particles involved in this reaction are not pointlike, we introduce hadron form factors to take their finite size into account. One of the greatest advantages of the approach employed in this work is the small number of the free parameters. As there are to this date no data available for the photoproduction of $\bar{D}^0\Lambda_c^+$, we had to rely on the broken SU(4) symmetry and other recent works to hint us at reasonable values of the otherwise unconstrained parameter $g_{D\Lambda_c^+N}$. The rest of the parameters were then adjusted by hand so that we could give at least some qualitative results. We thoroughly discuss the behavior of the Regge background with the pseudoscalar and pseudovector couplings in the strong vertex and reveal that the contact term, imitating the higher-order contributions, together with the s-channel proton exchange play a non-negligible role in the model predictions. As soon as the experimental data on this process become available, we will be able to utilize them not only for fitting the handful of free parameters but also for considering the correct phase of the Regge propagator, and thus providing a more thorough analysis of this process.

ACKNOWLEDGMENTS

The authors thank P. Bydžovský for fruitful discussions and useful comments. This work was supported in part by JSPS KAKENHI Grant No. JP20K14478 and Special Postdoctoral Researcher program of RIKEN (Y. Y.).

APPENDIX A: EFFECTIVE COUPLINGS OF A PHOTON AND D MESONS

In this Appendix, we summarize the derivation of the effective coupling of a photon and D mesons (γDD) via the VMD.

1. Effective Lagrangians

The amplitudes of a photon and pseudoscalar mesons (γPP) via the vector meson dominance are derived by the effective Lagrangians [38,83,105],

$$\mathcal{L} = \mathcal{L}_{\gamma V} + \mathcal{L}_{VPP} + \mathcal{L}_{\gamma PP}, \tag{A1}$$

where

$$\mathcal{L}_{\gamma V} = -\sqrt{2} e g_{\gamma V} A_\mu \mathrm{tr}(QV^\mu), \tag{A2}$$

$$\mathcal{L}_{VPP} = i2\sqrt{2} g_{VPP} \mathrm{tr}(V_\mu [\partial^\mu P, P]), \tag{A3}$$

$$\mathcal{L}_{\gamma PP} = ie\left(1 - \frac{a}{2}\right) A_\mu \mathrm{tr}(Q[\partial^\mu P, P]). \tag{A4}$$

The coupling constants are given by

$$g_{\gamma V} = \frac{m_V^2}{g_\gamma} \sim 0.10\ \mathrm{GeV}^2, \tag{A5}$$

$$g_{VPP} = \frac{g_\gamma a}{8} \sim 1.4, \tag{A6}$$

with $m_V = 770$ MeV, $g_\gamma = 5.7$, and $a = 2$ in the standard VMD model [38,83,105]. Thus, the direct γPP coupling (A4) vanishes, while pseudoscalar mesons couple to a photon via a vector-meson coupling. The SU(4) meson matrices are given by

$$P = \begin{pmatrix} \frac{\pi^0}{\sqrt{2}} + \frac{\eta}{\sqrt{6}} + \frac{\eta'}{\sqrt{3}} & \pi^+ & K^+ & \bar{D}^0 \\ \pi^- & -\frac{\pi^0}{\sqrt{2}} + \frac{\eta}{\sqrt{6}} + \frac{\eta'}{\sqrt{3}} & K^0 & D^- \\ K^- & \bar{K}^0 & -\frac{2\eta}{\sqrt{6}} + \frac{\eta'}{\sqrt{3}} & D_s^- \\ D^0 & D^+ & D_s^+ & \eta_c \end{pmatrix}, \tag{A7}$$

$$V_\mu = \begin{pmatrix} \frac{\rho^0}{\sqrt{2}} + \frac{\omega}{\sqrt{2}} & \rho^+ & K^{*+} & \bar{D}^{*0} \\ \rho^- & -\frac{\rho^0}{\sqrt{2}} + \frac{\omega}{\sqrt{2}} & K^{*0} & D^{*-} \\ K^{*-} & \bar{K}^{*0} & \phi & D_s^{*-} \\ D^{*0} & D^{*+} & D_s^{*+} & \psi \end{pmatrix}_\mu, \tag{A8}$$

and

$$Q = \frac{1}{3}\begin{pmatrix} 2 & 0 & 0 & 0 \\ 0 & -1 & 0 & 0 \\ 0 & 0 & -1 & 0 \\ 0 & 0 & 0 & 2 \end{pmatrix}. \tag{A9}$$

The Lagrangian $\mathcal{L}_{\gamma V}$ in (A2) yields couplings between a photon and neutral vector meson,

$$\mathcal{L}_{\gamma V^0} = -e g_{\gamma V} A_\mu \left(\rho^0 + \frac{1}{3}\omega - \frac{\sqrt{2}}{3}\phi + \frac{2\sqrt{2}}{3}\psi\right)^\mu. \tag{A10}$$

The Lagrangian $\mathcal{L}_{VPP}$ in (A3) yields couplings of a vector meson and pseudoscalar mesons. The γDD amplitudes are obtained by the couplings to a neutral vector meson which are given as

$$\begin{aligned} \mathcal{L}_{V^0DD} = i2g_{VPP}[&(\rho^0+\omega)_\mu(\partial^\mu\bar{D}^0 D^0 - \bar{D}^0\partial^\mu D^0) \\ &+ \sqrt{2}\psi_\mu(\partial^\mu D^0\bar{D}^0 - D^0\partial^\mu\bar{D}^0) \\ &+ (-\rho^0+\omega)_\mu(\partial^\mu D^- D^+ - D^-\partial^\mu D^+) \\ &+\sqrt{2}\psi_\mu(\partial^\mu D^+ D^- - D^+\partial^\mu D^-)] \end{aligned} \tag{A11}$$

for D mesons.

2. The γPP amplitudes in the SU(4) symmetry

From the Lagrangians derived in the previous subsection, the γPP couplings via the VMD are obtained.

For the D mesons, the amplitude of the γDD coupling is obtained as

$$\begin{aligned} &\langle \bar{D}^0(p_D)D^0(q)|i\mathcal{L}_{V^0\bar{D}^0D^0} i\mathcal{L}_{\gamma V^0}|\gamma(k)\rangle \\ &= -i2eg_{\gamma V}g_{VPP}\varepsilon\cdot(p_D-q)\left(\frac{1}{m_\rho^2}+\frac{1}{3m_\omega^2}-\frac{4}{3m_\psi^2}\right) \end{aligned} \tag{A12}$$

for neutral D mesons, and

$$\begin{aligned} &\langle D^-(p_D)D^+(q)|i\mathcal{L}_{V^0D^-D^+} i\mathcal{L}_{\gamma V^0}|\gamma(k)\rangle \\ &= i2eg_{\gamma V}g_{VPP}\varepsilon\cdot(p_D-q)\left(\frac{1}{m_\rho^2}-\frac{1}{3m_\omega^2}+\frac{4}{3m_\psi^2}\right) \end{aligned} \tag{A13}$$

for $D^\pm$ mesons. p_D^μ and q^μ are four-momenta of D mesons. k^μ is a four-momentum of a photon, and $k^2 = 0$ is used. ε^μ is a polarization vector of the photon. In the SU(4) limit with $m_V^2 = m_\rho^2 = m_\omega^2 = m_\psi^2$, the γDD amplitudes are reduced to

$$\langle \bar{D}^0(p_D)D^0(q)|i\mathcal{L}_{V^0\bar{D}^0D^0} i\mathcal{L}_{\gamma V^0}|\gamma(k)\rangle \xrightarrow[SU(4)\text{ limit}]{} 0, \tag{A14}$$

$$\begin{aligned} &\langle D^-(p_D)D^+(q)|i\mathcal{L}_{V^0D^-D^+} i\mathcal{L}_{\gamma V^0}|\gamma(k)\rangle \\ &\xrightarrow[SU(4)\text{ limit}]{} ie\varepsilon\cdot(p_D-q), \end{aligned} \tag{A15}$$

which are equal to amplitudes of neutral and charged pseudoscalar bosons. Introducing the physical hadron masses, $m_\rho = 770$ MeV, $m_\omega = 782$ MeV and $m_\psi = 3097$ MeV, the amplitudes are obtained as

$$\begin{aligned} &\langle \bar{D}^0(p_D)D^0(q)|i\mathcal{L}_{V^0\bar{D}^0D^0} i\mathcal{L}_{\gamma V^0}|\gamma(k)\rangle \\ &= -0.19ie\varepsilon\cdot(p_D-q), \end{aligned} \tag{A16}$$

$$\begin{aligned} &\langle D^-(p_D)D^+(q)|i\mathcal{L}_{V^0D^-D^+} i\mathcal{L}_{\gamma V^0}|\gamma(k)\rangle \\ &= 0.11ie\varepsilon\cdot(p_D-q), \end{aligned} \tag{A17}$$

where the strength of the γDD amplitude differs from the one in the SU(4) limit. We emphasize that introducing the physical hadron masses generate the nonzero $\gamma D^0 D^0$ coupling while it vanishes in the SU(4) limit. These amplitudes can be regarded as those obtained by the effective γDD Lagrangians

$$\mathcal{L}^{(SU(4))}_{\gamma\bar{D}^0D^0} = 0.19iA^\mu(\partial_\mu\bar{D}^0D^0 - \bar{D}^0\partial_\mu D^0), \tag{A18}$$

$$\mathcal{L}^{(SU(4))}_{\gamma D^-D^+} = -0.11iA^\mu(\partial_\mu D^-D^+ - D^-\partial_\mu D^+). \tag{A19}$$

3. The γDD amplitudes in the phenomenological model

In Sec. A 2, the flavor SU(4) symmetry is employed to determine the coupling constants for charmed mesons. However, this symmetry is broken due to the large mass of the charm quark. In this subsection, we introduce the phenomenological model to determine the coupling constants and obtain the amplitude of the γDD couplings.

The coupling constant of the $\gamma J/\psi$ coupling, $g_{\gamma\psi}$, can be determined by the $J/\psi \to e^+e^-$ decay [15], where

$$\Gamma(J/\psi \to e^+e^-) = \frac{16\pi\alpha^2}{27}\frac{2g_{\gamma\psi}^2}{m_\psi^3} = 5.55\text{ keV}. \tag{A20}$$

TABLE III. The coupling constants $g_{\psi DD}$ and the corresponding strength of the γDD effective Lagrangians, $C^{\gamma D^-D^+}$ and $C^{\gamma\bar{D}^0D^0}(=C^{(\mathrm{model})})$. The results obtained by the various models, the SU(4) symmetry (SU(4)), QCDSR, and the quark model, are shown.

Model	$g_{\psi DD}$	$C^{\gamma\bar{D}^0D^0}$	$C^{\gamma D^-D^+}$	Reference
SU(4)	$g_{VPP}=1.4$	0.15	0.23	[105]
QCDSR	2.9	0.036	0.36	[107]
Quark model	4.6	−0.093	0.48	[108]

Then, $|g_{\gamma\psi}|=0.91\ \mathrm{GeV}^2$ is obtained, which is much larger than $g_{\gamma V}\sim 0.10\ \mathrm{GeV}^2$ in (A5).

For the ρDD and ωDD couplings, the heavy meson effective theory is employed, where

$$g_{VDD}=\frac{\beta g_V}{2\sqrt{2}}=1.9 \tag{A21}$$

with $\beta=0.9$ and $g_V=5.8$ [106]. The $J/\psi DD$ coupling constant is obtained by model calculations such as the QCDSR and the quark model as summarized in Table III, while these results are not consistent with each other.

The amplitudes of the γDD couplings are obtained as

$$\begin{aligned}&\langle\bar{D}^0(p_D)D^0(q)|i\mathcal{L}_{V^0\bar{D}^0D^0}i\mathcal{L}_{\gamma V^0}|\gamma(k)\rangle\\&=-i2\left[g_{\gamma V}g_{VDD}\left(\frac{1}{m_\rho^2}+\frac{1}{3m_\omega^2}\right)-\frac{4}{3}\frac{g_{\gamma\psi}g_{\psi DD}}{m_\psi^2}\right]e\varepsilon\cdot(p_D-q)\\&\equiv -iC^{\gamma\bar{D}^0D^0}\varepsilon\cdot(p_D-q),\end{aligned} \tag{A22}$$

$$\begin{aligned}&\langle D^-(p_D)D^+(q)|i\mathcal{L}_{V^0D^-D^+}i\mathcal{L}_{\gamma V^0}|\gamma(k)\rangle\\&=i2\left[g_{\gamma V}g_{VDD}\left(\frac{1}{m_\rho^2}-\frac{1}{3m_\omega^2}\right)+\frac{4}{3}\frac{g_{\gamma\psi}g_{\psi DD}}{m_\psi^2}\right]e\varepsilon\cdot(p_D-q)\\&\equiv iC^{\gamma D^-D^+}\varepsilon\cdot(p_D-q),\end{aligned} \tag{A23}$$

where the constant $C^{\gamma\bar{D}^0D^0}$ ($C^{\gamma D^-D^+}$) is given by 0.15 (0.23) for the SU(4) model, 0.036 (0.36) for $g_{\psi DD}=2.9$ the QCDSR, and −0.093 (0.48) for the quark model as summarized in Table III. The constant $C^{(\mathrm{model})}$ used in Eq. (17) above is given as $C^{(\mathrm{model})}\equiv C^{\gamma\bar{D}^0D^0}$, where model = SU(4), QCDSR, quark model.

The effective Lagrangians which yield the amplitudes (A22) and (A23) can be written by

$$\mathcal{L}^{(\mathrm{ph})}_{\gamma\bar{D}^0D^0}=iC^{\gamma\bar{D}^0D^0}A^\mu(\partial_\mu\bar{D}^0D^0-\bar{D}^0\partial_\mu D^0), \tag{A24}$$

$$\mathcal{L}^{(\mathrm{ph})}_{\gamma D^-D^+}=-iC^{\gamma D^-D^+}A^\mu(\partial_\mu D^-D^+-D^-\partial_\mu D^+), \tag{A25}$$

where $C^{\gamma\bar{D}^0D^0}$ and $C^{\gamma D^-D^+}$ are regarded as the coupling constants of the effective γDD Lagrangians.

APPENDIX B: TRANSFORMATION MATRIX OF THE GAUGE-INVARIANT OPERATORS

In the paper of Levy *et al.* [95,96], the authors use a different basis to ours for the gauge-invariant operators. We denote the gauge-invariant operators in their basis $\mathcal{M}_i^L$ and they read

$$\mathcal{M}_1^L=\frac{1}{2}\gamma_5(\not{\varepsilon}\not{k}-\not{k}\not{\varepsilon}), \tag{B1a}$$

$$\mathcal{M}_2^L=2\gamma_5(p_K\cdot\varepsilon P\cdot k-p_K\cdot kP\cdot\varepsilon), \tag{B1b}$$

$$\mathcal{M}_3^L=\gamma_5(\not{\varepsilon}p_K\cdot k-\not{k}p_K\cdot\varepsilon), \tag{B1c}$$

$$\mathcal{M}_4^L=i\epsilon_{\alpha\beta\mu\nu}\gamma^\alpha p_K^\beta\varepsilon^\mu k^\nu, \tag{B1d}$$

$$\mathcal{M}_5^L=\gamma_5(p_K\cdot\varepsilon k^2-p_K\cdot kk\cdot\varepsilon), \tag{B1e}$$

$$\mathcal{M}_6^L=\gamma_5(k\cdot\varepsilon\not{k}-k^2\not{\varepsilon}). \tag{B1f}$$

The gauge-invariant operators $\mathcal{M}_i^L$ in the basis of Levy *et al.* [95,96] can be rewritten in terms of gauge-invariant operators $\mathcal{M}_i$ of our basis, shown in Eq. (A5), as

$$\mathcal{M}_1^L=-\gamma_5\mathcal{M}_1, \tag{B2a}$$

$$\mathcal{M}_2^L=\gamma_5[(2p_\Lambda\cdot k-k^2)\mathcal{M}_2-(2p\cdot k+k^2)\mathcal{M}_3], \tag{B2b}$$

$$\mathcal{M}_3^L=\gamma_5(\mathcal{M}_4-\mathcal{M}_5-\mathcal{M}_6), \tag{B2c}$$

$$\mathcal{M}_4^L=\gamma_5[-(m_\Lambda+m_p)\mathcal{M}_1-\mathcal{M}_4-\mathcal{M}_5], \tag{B2d}$$

$$\mathcal{M}_5^L=\gamma_5k^2(\mathcal{M}_2-\mathcal{M}_3), \tag{B2e}$$

$$\mathcal{M}_6^L=\gamma_5\mathcal{M}_6. \tag{B2f}$$

From here, we can schematically write the transition between these two bases, i.e., $\mathcal{M}_i^L=\gamma_5R_j^i\mathcal{M}_j$, where the transformation matrix reads

$$R_j^i=\begin{pmatrix}-1 & 0 & 0 & 0 & 0 & 0\\ 0 & 2k\cdot p_\Lambda-k^2 & -2k\cdot p-k^2 & 0 & 0 & 0\\ 0 & 0 & 0 & 1 & -1 & -1\\ -m_\Lambda-m_p & 0 & 0 & -1 & -1 & 0\\ 0 & k^2 & -k^2 & 0 & 0 & 0\\ 0 & 0 & 0 & 0 & 0 & 1\end{pmatrix}. \tag{B3}$$

[1] E. S. Swanson, Phys. Rep. **429**, 243 (2006).
[2] N. Brambilla *et al.*, Eur. Phys. J. C **71**, 1534 (2011).
[3] A. Hosaka, T. Iijima, K. Miyabayashi, Y. Sakai, and S. Yasui, Prog. Theor. Exp. Phys. **2016**, 062C01 (2016).
[4] Y. Yamaguchi, A. Hosaka, S. Takeuchi, and M. Takizawa, J. Phys. G **47**, 053001 (2020).
[5] T. Yoshida, E. Hiyama, A. Hosaka, M. Oka, and K. Sadato, Phys. Rev. D **92**, 114029 (2015).
[6] Y. Kato and T. Iijima, Prog. Part. Nucl. Phys. **105**, 61 (2019).
[7] M. Harada, Y. R. Liu, M. Oka, and K. Suzuki, Phys. Rev. D **101**, 054038 (2020).
[8] Y. Kim, E. Hiyama, M. Oka, and K. Suzuki, Phys. Rev. D **102**, 014004 (2020).
[9] N. Isgur and M. B. Wise, Phys. Lett. B **232**, 113 (1989).
[10] N. Isgur and M. B. Wise, Phys. Lett. B **237**, 527 (1990).
[11] N. Isgur and M. B. Wise, Phys. Rev. Lett. **66**, 1130 (1991).
[12] M. Neubert, Phys. Rep. **245**, 259 (1994).
[13] A. V. Manohar and M. B. Wise, *Heavy Quark Physics*, Cambridge Monographs on Particle Physics, Nuclear Physics and Cosmology (Cambridge University Press, Cambridge, England, 2000), p. 191.
[14] A. Hosaka, T. Hyodo, K. Sudoh, Y. Yamaguchi, and S. Yasui, Prog. Part. Nucl. Phys. **96**, 88 (2017).
[15] M. Tanabashi *et al.* (Particle Data Group), Phys. Rev. D **98**, 030001 (2018).
[16] A. J. Bevan *et al.* (*BABAR* and Belle Collaborations), Eur. Phys. J. C **74**, 3026 (2014).
[17] C. Z. Yuan and S. L. Olsen, Nat. Rev. Phys. **1**, 480 (2019).
[18] R. Aaij *et al.* (LHCb Collaboration), Eur. Phys. J. C **72**, 1972 (2012).
[19] R. Aaij *et al.* (LHCb Collaboration), Phys. Rev. Lett. **112**, 222002 (2014).
[20] R. Aaij *et al.* (LHCb Collaboration), Phys. Rev. Lett. **115**, 072001 (2015).
[21] R. Aaij *et al.* (LHCb Collaboration), Phys. Rev. Lett. **117**, 082002 (2016).
[22] R. Aaij *et al.* (LHCb Collaboration), Phys. Rev. Lett. **117**, 082003 (2016); **117**, 109902(A) (2016); **118**, 119901(A) (2017).
[23] R. Aaij *et al.* (LHCb Collaboration), Phys. Rev. Lett. **122**, 222001 (2019).
[24] R. Aaij *et al.* (LHCb Collaboration), Phys. Rev. Lett. **123**, 152001 (2019).
[25] R. Aaij *et al.* (LHCb Collaboration), Phys. Rev. Lett. **124**, 082002 (2020).
[26] R. Aaij *et al.* (LHCb Collaboration), J. High Energy Phys. 06 (2020) 136.
[27] R. Aaij *et al.* (LHCb Collaboration), Phys. Rev. Lett. **124**, 222001 (2020).
[28] A. Ali *et al.* (GlueX Collaboration), Phys. Rev. Lett. **123**, 072001 (2019).
[29] Z. E. Meziani *et al.*, arXiv:1609.00676; Erratum, https://www.jlab.org/exp_prog/proposals/16/PR12-16-007-erratum.pdf.
[30] H. Noumi *et al.*, Charmed baryon spectroscopy via the (π, D^{*-}) reaction, http://j-parc.jp/researcher/Hadron/en/pac_1301/pdf/P50_2012-19.pdf.
[31] H. X. Chen, W. Chen, X. Liu, and S. L. Zhu, Phys. Rep. **639**, 1 (2016).
[32] A. Ali, J. S. Lange, and S. Stone, Prog. Part. Nucl. Phys. **97**, 123 (2017).
[33] Y. R. Liu, H. X. Chen, W. Chen, X. Liu, and S. L. Zhu, Prog. Part. Nucl. Phys. **107**, 237 (2019).
[34] S. G. Yuan, K. W. Wei, J. He, H. S. Xu, and B. S. Zou, Eur. Phys. J. A **48**, 61 (2012).
[35] S. Takeuchi and M. Takizawa, Phys. Lett. B **764**, 254 (2017).
[36] E. Santopinto and A. Giachino, Phys. Rev. D **96**, 014014 (2017).
[37] J. J. Wu, R. Molina, E. Oset, and B. S. Zou, Phys. Rev. Lett. **105**, 232001 (2010).
[38] J. J. Wu, R. Molina, E. Oset, and B. S. Zou, Phys. Rev. C **84**, 015202 (2011).
[39] C. Garcia-Recio, J. Nieves, O. Romanets, L. L. Salcedo, and L. Tolos, Phys. Rev. D **87**, 074034 (2013).
[40] M. Karliner and J. L. Rosner, Phys. Rev. Lett. **115**, 122001 (2015).
[41] R. Chen, X. Liu, X. Q. Li, and S. L. Zhu, Phys. Rev. Lett. **115**, 132002 (2015).
[42] L. Roca, J. Nieves, and E. Oset, Phys. Rev. D **92**, 094003 (2015).
[43] J. He, Phys. Lett. B **753**, 547 (2016).
[44] U. G. Meißner and J. A. Oller, Phys. Lett. B **751**, 59 (2015).
[45] H. X. Chen, W. Chen, X. Liu, T. G. Steele, and S. L. Zhu, Phys. Rev. Lett. **115**, 172001 (2015).
[46] T. Uchino, W. H. Liang, and E. Oset, Eur. Phys. J. A **52**, 43 (2016).
[47] T. J. Burns, Eur. Phys. J. A **51**, 152 (2015).
[48] Y. Yamaguchi and E. Santopinto, Phys. Rev. D **96**, 014018 (2017).
[49] Y. Yamaguchi, A. Giachino, A. Hosaka, E. Santopinto, S. Takeuchi, and M. Takizawa, Phys. Rev. D **96**, 114031 (2017).
[50] Y. Shimizu, D. Suenaga, and M. Harada, Phys. Rev. D **93**, 114003 (2016).
[51] Y. Shimizu and M. Harada, Phys. Rev. D **96**, 094012 (2017).
[52] Y. Shimizu, Y. Yamaguchi, and M. Harada, Phys. Rev. D **98**, 014021 (2018).
[53] Y. Shimizu, Y. Yamaguchi, and M. Harada, Prog. Theor. Exp. Phys. **2019**, 123D01 (2019).
[54] J. J. Wu and B. S. Zou, Phys. Lett. B **709**, 70 (2012).
[55] C. W. Xiao and E. Oset, Eur. Phys. J. A **49**, 139 (2013).
[56] K. Azizi, Y. Sarac, and H. Sundu, Phys. Rev. D **96**, 094030 (2017).
[57] H. X. Chen, W. Chen, and S. L. Zhu, Phys. Rev. D **100**, 051501(R) (2019).
[58] C. W. Xiao, J. Nieves, and E. Oset, Phys. Rev. D **100**, 014021 (2019).
[59] M. Z. Liu, Y. W. Pan, F. Z. Peng, M. Sánchez Sánchez, L. S. Geng, A. Hosaka, and M. Pavon Valderrama, Phys. Rev. Lett. **122**, 242001 (2019).
[60] Y. Shimizu, Y. Yamaguchi, and M. Harada, arXiv:1904.00587.
[61] F. Giannuzzi, Phys. Rev. D **99**, 094006 (2019).
[62] J. F. Giron, R. F. Lebed, and C. T. Peterson, J. High Energy Phys. 05 (2019) 061.
[63] J. He, Eur. Phys. J. C **79**, 393 (2019).

[64] A. Ali and A. Y. Parkhomenko, Phys. Lett. B **793**, 365 (2019).
[65] Z. H. Guo and J. A. Oller, Phys. Lett. B **793**, 144 (2019).
[66] Y. Yamaguchi, H. García-Tecocoatzi, A. Giachino, A. Hosaka, E. Santopinto, S. Takeuchi, and M. Takizawa, Phys. Rev. D **101**, 091502(R) (2020).
[67] T. J. Burns and E. S. Swanson, Phys. Rev. D **100**, 114033 (2019).
[68] Y. Huang, J. He, H. F. Zhang, and X. R. Chen, J. Phys. G **41**, 115004 (2014).
[69] V. Kubarovsky and M. B. Voloshin, Phys. Rev. D **92**, 031502(R) (2015).
[70] Q. Wang, X. H. Liu, and Q. Zhao, Phys. Rev. D **92**, 034022 (2015).
[71] A. N. H. Blin, C. Fernández-Ramírez, A. Jackura, V. Mathieu, V. I. Mokeev, A. Pilloni, and A. P. Szczepaniak, Phys. Rev. D **94**, 034002 (2016).
[72] Y. Huang, J. J. Xie, J. He, X. Chen, and H. F. Zhang, Chin. Phys. C **40**, 124104 (2016).
[73] J. J. Wu, T.-S. H. Lee, and B. S. Zou, Phys. Rev. C **100**, 035206 (2019).
[74] X. Cao, F. K. Guo, Y. T. Liang, J. J. Wu, J. J. Xie, Y. P. Xie, Z. Yang, and B. S. Zou, Phys. Rev. D **101**, 074010 (2020).
[75] Z. Yang, X. Cao, Y. T. Liang, and J. J. Wu, Chin. Phys. C **44**, 084102 (2020).
[76] E. J. Garzon and J. J. Xie, Phys. Rev. C **92**, 035201 (2015).
[77] X. H. Liu and M. Oka, Nucl. Phys. **A954**, 352 (2016).
[78] S. H. Kim, H. C. Kim, and A. Hosaka, Phys. Lett. B **763**, 358 (2016).
[79] C. Cheng and X. Y. Wang, Adv. High Energy Phys. **2017**, 9398732 (2017).
[80] P. Bydžovský and D. Skoupil, Phys. Rev. C **100**, 035202 (2019).
[81] T. Corthals, J. Ryckebusch, and T. Van Cauteren, Phys. Rev. C **73**, 045207 (2006).
[82] J. Sakurai, Ann. Phys. (N.Y.) **11**, 1 (1960).
[83] M. Harada and K. Yamawaki, Phys. Rep. **381**, 1 (2003).
[84] U. Wiedner, Prog. Part Nucl. Phys. **66**, 477 (2011).
[85] S. Janssen, Ph.D. thesis, Ghent University, 2002.
[86] Y. Oh, W. Liu, and C. M. Ko, Phys. Rev. C **75**, 064903 (2007).
[87] F. S. Navarra and M. Nielsen, Phys. Lett. B **443**, 285 (1998).
[88] F. O. Duraes, F. S. Navarra, and M. Nielsen, Phys. Lett. B **498**, 169 (2001).
[89] K. Azizi, Y. Sarac, and H. Sundu, Phys. Rev. D **90**, 114011 (2014).
[90] A. Khodjamirian, C. Klein, T. Mannel, and Y.-M. Wang, J. High Energy Phys. 09 (**2011**) 106.
[91] C. E. Fontoura, J. Haidenbauer, and G. Krein, Eur. Phys. J. A **53**, 92 (2017).
[92] D. Skoupil and P. Bydžovský, Phys. Rev. C **93**, 025204 (2016).
[93] R. A. Williams, C. R. Ji, and S. R. Cotanch, Phys. Rev. C **46**, 1617 (1992).
[94] F. A. Berends, A. Donnachie, and D. L. Weaver, Nucl. Phys. **B4**, 1 (1967).
[95] N. Levy, W. Majerotto, and B. J. Read, Nucl. Phys. **B55**, 493 (1973).
[96] N. Levy, W. Majerotto, and B. J. Read, Nucl. Phys. **B55**, 513 (1973).
[97] M. Sotona and S. Frullani, Prog. Theor. Phys. Suppl. **117**, 151 (1994).
[98] J. C. David, C. Fayard, G.-H. Lamot, and B. Saghai, Phys. Rev. C **53**, 2613 (1996).
[99] L. De Cruz, Bayesian model selection for electromagnetic kaon productionin the Regge-plus-resonance framework, Ph.D. thesis, Ghent University, 2010.
[100] A. Capella and J. T. V. Thanh, Lett. Nuovo Cimento **4**, 1199 (1970).
[101] J. Tran Thanh Van, J. Phys. (Paris), Colloq. **32**, C3 (1971), https://inspirehep.net/literature/1396383.
[102] A. S. Fomin, S. Barsuk, A. Yu. Korchin, E. Kou, V. A. Kovalchuk, M. Liul, A. Natochii, E. Niel, P. Robbe, and A. Stocchi Eur. Phys. J. C **80**, 358 (2020).
[103] M. Guidal, J.-M. Laget, and M. Vanderhaeghen, Nucl. Phys. **A627**, 645 (1997).
[104] H. Haberzettl, X. Y. Wang, and J. He, Phys. Rev. C **92**, 055503 (2015).
[105] F. Klingl, N. Kaiser, and W. Weise, Z. Phys. A **356**, 193 (1996).
[106] Y. Yamaguchi, S. Ohkoda, S. Yasui, and A. Hosaka, Phys. Rev. D **84**, 014032 (2011).
[107] R. D. Matheus, F. Navarra, M. Nielsen, and R. Rodrigues da Silva, Phys. Lett. B **541**, 265 (2002).
[108] W. Lucha, D. Melikhov, H. Sazdjian, and S. Simula, Phys. Rev. D **93**, 016004 (2016).